AD-A114 492 CHARLES STARK DRAPER LAB INC CAMBRIDGE MA F/G 8/10
OCEAN ACOUSTIC TOMOGRAPHY MOORING DESIGN STUDY.(U)
APR 82 J R SCHOLTEN, N K CHHABRA N00014-75-C-0291
UNCLASSIFIED R-1555 NL

1 OF 1
ADA
114492

END
DATE
FILMED
06-82
DTIC

AD A114492

R-1555

Ocean Acoustic Tomography Mooring Design Study

by

James R. Scholten
and
Narender K. Chhabra

The Charles Stark Draper Laboratory, Inc.
Cambridge, Massachusetts 02139

Approved for public release; distribution unlimited.

82 05 14 044

SECURITY CLASSIFICATION OF THIS PAGE (When Data Entered)

REPORT DOCUMENTATION PAGE		READ INSTRUCTIONS BEFORE COMPLETING FORM
1. REPORT NUMBER	2. GOVT ACCESSION NO. AD-A114 492	3. RECIPIENT'S CATALOG NUMBER
4. TITLE (and Subtitle) OCEAN ACOUSTIC TOMOGRAPHY MOORING DESIGN STUDY		5. TYPE OF REPORT & PERIOD COVERED Technical Report
		6. PERFORMING ORG. REPORT NUMBER R-1555
7. AUTHOR(s) James R. Scholten Narender K. Chhabra		8. CONTRACT OR GRANT NUMBER(s) N00014-75-C-0291
9. PERFORMING ORGANIZATION NAME AND ADDRESS The Charles Stark Draper Laboratory, Inc. Cambridge, Massachusetts 02139		10. PROGRAM ELEMENT, PROJECT, TASK AREA & WORK UNIT NUMBERS
11. CONTROLLING OFFICE NAME AND ADDRESS Office of Naval Research, Code 480 800 North Quincy Street Arlington, VA 22217		12. REPORT DATE April 1982
		13. NUMBER OF PAGES 82
14. MONITORING AGENCY NAME & ADDRESS (if different from Controlling Office)		15. SECURITY CLASS. (of this report) Unclassified
		15a. DECLASSIFICATION/DOWNGRADING SCHEDULE

16. DISTRIBUTION STATEMENT (of this Report)

Approved for public release; distribution unlimited.

17. DISTRIBUTION STATEMENT (of the abstract entered in Block 20, if different from Report)

18. SUPPLEMENTARY NOTES

19. KEY WORDS (Continue on reverse side if necessary and identify by block number)

Ocean moorings
Acoustic tomography

20. ABSTRACT (Continue on reverse side if necessary and identify by block number)

Ocean Acoustic Tomograpy requires deep-ocean moorings whose horizontal excursions are either small or accurately measured. The present study rigorously investigates the former case: the design of stiff moorings to meet any particular horizontal excursion goal (e.g., 25 meters) under two typical ocean current-versus-depth profiles. Moorings are considered for tomographic transmitters and receivers at depths ranging from one thousand to four thousand meters. Mooring components considered include

DD FORM 1 JAN 73 1473 EDITION OF 1 NOV 65 IS OBSOLETE

SECURITY CLASSIFICATION OF THIS PAGE (When Data Entered)

steel sphere, glass ball, and syntactic foam buoyancy; jacketed 3x19 wire and electromagnetic cable; and a realistic (large) battery pack for the acoustic transmitter. Kevlar mooring line was considered and rejected.

The basic tool of this study is a well-verified computer program that simulates mooring motion. Many runs of this program have yielded enough data to make plots showing mooring cost as a function of excursion, depth, and mooring type. It has been found that cost and excursion are very sensitive to the current profile. For moderate currents (15 cm/sec), placing instruments at lesser depths (1000-2000 m) is expensive ($50,000 to $100,000 for wire and buoyancy alone). Deep deployments are much less expensive (about $15,000).

Given in appendices are studies of the computer simulation of ocean internal wave currents, power systems for the long-range acoustic transmitter, and a hypothetical steel sphere for subsurface buoyancy. Also given are tables of mooring component characteristics.

R-1555

OCEAN ACOUSTIC TOMOGRAPHY MOORING DESIGN STUDY

by

James R. Scholten

and

Narender K. Chhabra

The Charles Stark Draper Laboratory, Inc.
Cambridge, Massachusetts 02139

ACKNOWLEDGMENT

The authors gratefully thank the members of the Oceanography group at Draper Laboratory and our friends at the Massachusetts Institute of Technology for their continuing support and encouragement.

At CSDL we are especially indebted to John Dahlen for conceiving the mooring design approaches studied herein, and for guidance and invaluable advice on numerous occasions. To him and to John Shillingford goes credit for the study of power systems for the long-range acoustic transmitter. At MIT, Robert Heinmiller and Charles Eriksen lent us their experience concerning current profiles and related matters.

Particular thanks are due to Ms. Catherine Hall for her patient labor in preparing the manuscript.

This report was prepared by The Charles Stark Draper Laboratory, Inc. under subcontract SR213998 with the Massachusetts Institute of Technology, operating under grant OCE-8017791 from the National Science Foundation.

The work was also supported by the Office of Naval Research, Ocean Science and Technology Division, via contract N00014-75-C-0291 with the Massachusetts Institute of Technology and subcontract SR103434 with the Draper Laboratory

ABSTRACT

Ocean Acoustic Tomography requires deep-ocean moorings whose horizontal excursions are either small or accurately measured. The present study rigorously investigates the former case: the design of stiff moorings to meet any particular horizontal excursion goal (e.g., 25 meters) under two typical ocean current-versus-depth profiles. Moorings are considered for tomographic transmitters and receivers at depths ranging from one thousand to four thousand meters. Mooring components considered include steel sphere, glass ball, and syntactic foam buoyancy; jacketed 3 x 19 wire and electromagnetic cable; and a realistic (large) battery pack for the acoustic transmitter. Kevlar mooring line was considered and rejected.

The basic tool of this study is a well-verified computer program that simulates mooring motion. Many runs of this program have yielded enough data to make plots showing mooring cost as a function of excursion, depth, and mooring type. It has been found that cost and excursion are very sensitive to the current profile. For moderate currents (15 cm/sec), placing instruments at lesser depths (1000-2000 m) is expensive ($50,000 to $100,000 for wire and buoyancy alone). Deep deployments are much less expensive (about $15,000).

Given in appendices are studies of the computer simulation of ocean internal wave currents, power systems for the long-range acoustic transmitter, and a hypothetical steel sphere for subsurface buoyancy. Also given are tables of mooring component characteristics.

BLANK PAGE

TABLE OF CONTENTS

[illegible]

I. INTRODUCTION

A. Ocean Acoustic Tomography

Ocean Acoustic Tomography has great promise as a means to monitor the internal "weather" of the ocean. By measuring acoustic transmissions between many moorings over large distances ($\sim$ 1000 km), and deconvoluting by computer, density resolution of about 100 kilometers should be possible. Furthermore, depth resolution should be obtainable by discriminating acoustic multipaths between source (Long Range Transmitter, LRT) and receiver. For a detailed discussion on Ocean Acoustic Tomography and its capabilities see Munk and Wunsch (1979).

There are two obvious sources of error that must be strictly limited if tomographic acoustic travel times are to be meaningful. The first is clock drift between source and receiver, which must be less than about 25 milliseconds per year. The second is motion of the moored sources and receivers - any change in separation of over 25 meters must be accurately known so that travel times can be corrected.

This position-keeping requirement can be met in two ways; either the moorings can be acoustically tracked by ocean bottom-mounted transducers, or else the mooring can be built so stiffly that its excursion will rarely exceed the tolerable limits. The latter method is much simpler than the former, even if it must include an alarm sensor to warn of occasional excessive motion caused by abnormally high currents. However, because of unfavorable scaling ratios, stiff moorings can be massive and expensive to build. It is one purpose of the present study to quantitatively say how massive and how expensive.

B. Background

The main thrust of the study presented in this report was to perform preliminary mooring system design for the first large area experiment, tentatively planned for 1985. Figure 1 is a functional family tree illustrating the moored sensor system's role in relation to the other elements of the 1985 ocean acoustic tomography system.

The tool used to determine optimal mooring designs is computer simulation. Over the past few years the authors have created a set of computer simulations to model mooring mechanics (CHHABRA 1973, CHHABRA 1976, CHHABRA 1977A). These programs have been verified experimentally (CHHABRA 1974, CHHABRA 1977B, CHHABRA 1979, CHHABRA et al, 1974). For the present study the simulation is used for two things: (1) To determine mooring line safety factors, not only in the normal final deployed state but also during an anchor-last deployment free-fall. (2) To predict the quasi-static 3-dimensional deflection of the mooring under any given current vs. depth profile. The simulation has been used to design various source and/or receiver moorings that meet the tomographic excursion requirement for some reasonable current profiles.

The costs of these moorings have been tabulated, based on approximate dollar prices as of late 1980. Plots have been produced of cost vs. excursion and cost vs. source/receiver depth, all for an assortment of mooring configurations. The details of this work follow in the main body of this report.

As a by-product of this study, some results of wider interest have been obtained. These are detailed in appendices, and include:

(1) how to synthesize scientifically reasonable current profile histories, comprising mean uniform,

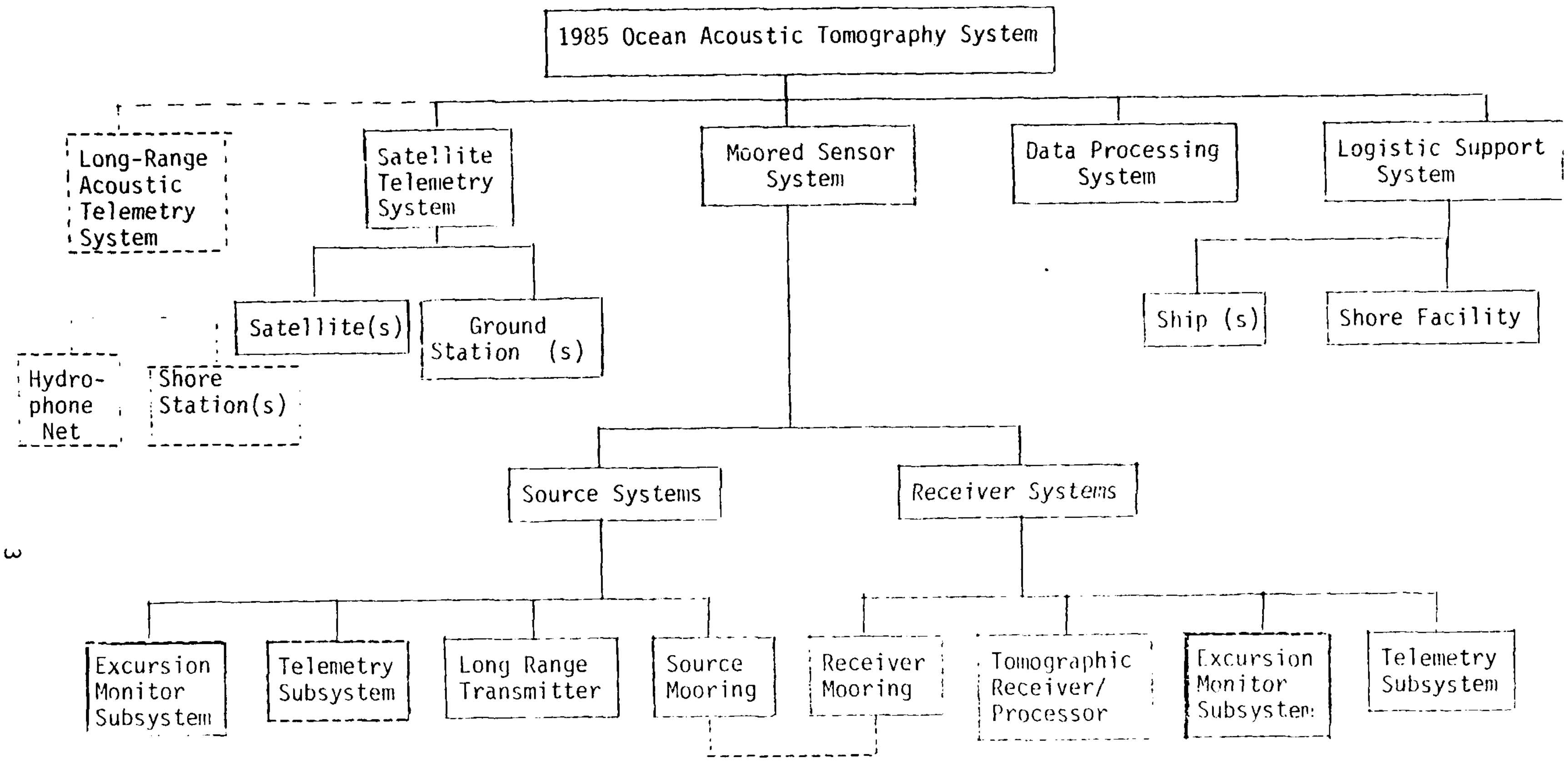

FUNCTIONAL FAMILY TREE

Figure 1

mean shear, tidal, inertial, and internal wave components. (Appendix A)

(2) a study of possible power systems for the Long Range acoustic Transmitter. (Appendix B)

(3) a detailed set of tables of mooring component characteristics. (Appendix C)

(4) a theoretical study of the cost and weight of ideal steel sphere buoys as a function of working depth. (Appendix D)

II. MOORED SENSOR SYSTEM GOALS AND SPECIFICATIONS

A. Scientific Requirements

For tomographic data to be scientifically useful, tomography moorings must meet exacting requirements. A tentative definition of these is given in Table 1. The most challenging of the specifications are the two-year lifetime, the real-time data telemetry, and the 25-meter horizontal excursion uncertainty limits on transmitters and receivers. The present report concentrates on the last of these problems.

The lifetime problem is addressed by the explicit sizing of a power system for the Long Range Transmitter (LRT), and by implicitly choosing other components with a two-year lifetime in mind. A study of real-time data telemetry is not included in this report; a hardware design study of satellite telemetry via a pop-up-buoy, which rests safely nested atop a subsurface moored buoy except during brief periods every few days when it surfaces to transmit data, is presented in DAHLEN et al. 1981.

An obvious approach to reducing excursion uncertainties is simply to stiffen (increase tension in) the mooring until the maximum excursion of the instrument is less than the allowed uncertainty. This solution is generally possible because line tensile strength increases with its diameter squared while line drag increases only linearly with diameter. However, because line weight also increases with diameter squared, a law of diminishing returns eventually takes hold to forbid arbitrarily low excursions. Of course, reliance upon this stiff mooring approach presumes a priori knowledge of at least the gross features of typical strong current profiles at the mooring site. It may also be necessary to provide an alarm to warn

1985 OCEAN ACOUSTIC TOMOGRAPHY SYSTEM SPECIFICATIONS

	Source Mooring	Receiver Mooring
Source/Receiver Horizontal Excursion		
Maximum Allowable Uncertainty	±25 meters	±25 meters
Source/Receiver Vertical Position		
Depth Error	±25 meters	±25 meters
Depth Uncertainty	±15 meters	±15 meters
Depth Range	1000-4500 m	1000-3500 m
Off-Bottom Height Range	>1000 meters	>1000 meters
Data Telemetry		
Minimum Interval between Messages		3 days
Binary Bits per Message		3000
Unattended Lifetime	2 years	2 years
Current Profile		
Typical 1	see Figure 2	
Typical 2	see Figure 3	

TABLE 1.

of the occasional occurrences of extreme profiles which push the mooring beyond the tolerable excursion. A brief survey of sensors suitable for this warning is presented in Section D of this chapter.

Another approach to reducing excursion uncertainties is active position tracking. A relatively soft mooring could be equipped with a comprehensive excursion monitoring system, designed to measure both the magnitude and direction of excursions to better than 25 meters accuracy. The most likely system to do this would involve acoustic ranging between the source or receiver and transponsders on the ocean floor nearby. Ideally a correction for each source-receiver pair would be computed in real-time by the receiver; to do this it would have to know the source's position, sent either by telemetry or else coded into the long-range acoustic signal itself. Less rigorous correction, perhaps using average position and/or post-processing, etc., may also be sufficient.

B. Current Profiles

The mooring motion study uses two profiles, illustrated in Figures 2 and 3.

Note that we have not included high order shear or any inertial or internal wave components, since a crude profile serves just as well as a complex one for comparing mooring excursions. If we wanted to simulate time histories of mooring <u>velocity</u>, then a full complexity profile would be needed. To this end we have written a computer program to synthesize inertial and internal wave currents, using a rigorous Garrett-Munk spectrum (see Appendix A).

C. Power System for the Long Range Transmitter

This item earns special consideration because of large mass and cost, and because of the lack of engineering

CURRENT PROFILE NO. 1

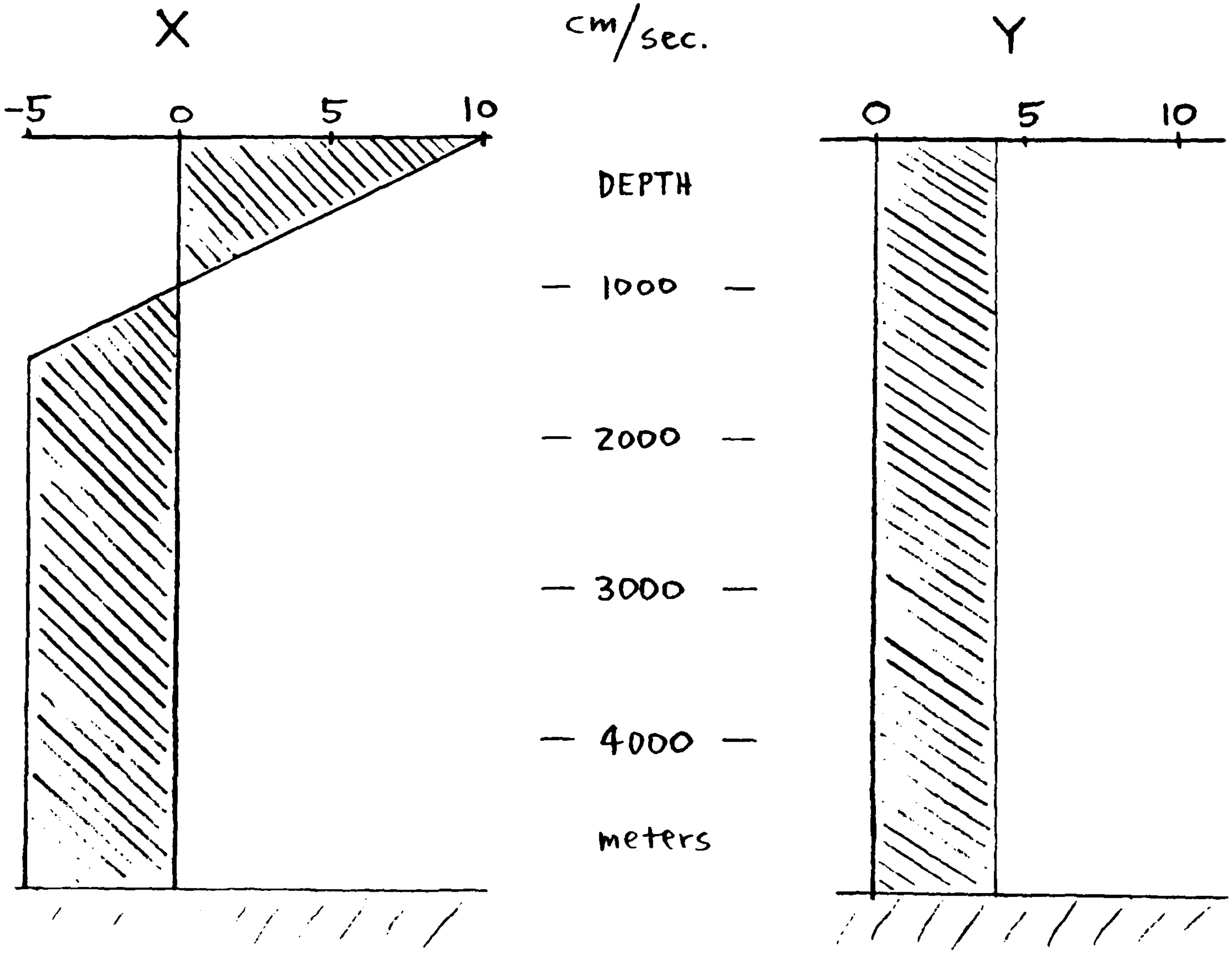

Figure 2

CURRENT PROFILE NO. 2

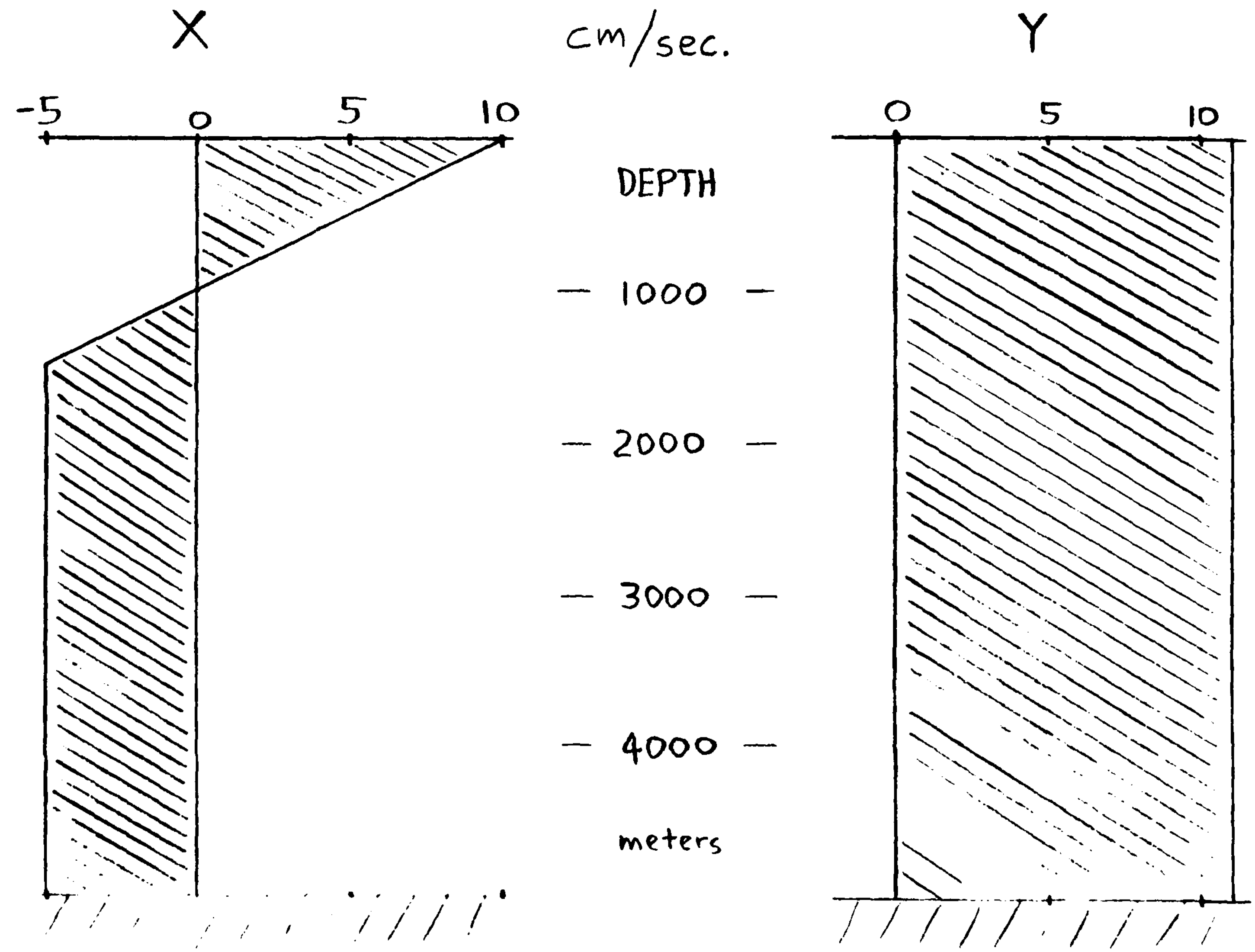

Figure 3

attention given it until now. In contrast, the acoustic Receiver and Long Range Transmitter are under development elsewhere and are in this report considered merely as black boxes of given size and weight.

The LRT power system options can perhaps best be summarized in a family tree, drawn in Figure 4. All power system options assume an energy requirement of 85 kilowatt-hours, based on a two-year life. Two strawman designs for a transmitter battery are sized in Appendix B.

D. Alarm Sensors

In the stiff mooring approach, each mooring would be equipped with a relatively simple excursion monitor to signal an alarm during the occasional high current event. On a receiver mooring this alarm would be telemetered along with the data. On a source-only mooring this alarm could be sounded by the LRT, possibly by a sequence of omissions, if a satellite link were not available. Most likely the alarm would be based upon a 3-day excursion averaging scheme. Alarm sensors considered are: pressure, current magnitude, current vector, inclination magnitude, inclination vector, and tension.

Pressure Sensor

A simple calculation of depth excursion for a given horizontal excursion and mooring line length gives

$$\Delta h = x^2/2\ell$$

Where: Δh is the depth excursion, x is the horizontal excursion and ℓ is the mooring length. For a 2000 m mooring with 25 m horizontal excursion Δh is 16 cm. This seems impractical to measure because 1) the resolution of the pressure sensor would have to be less than 10 centimeters,

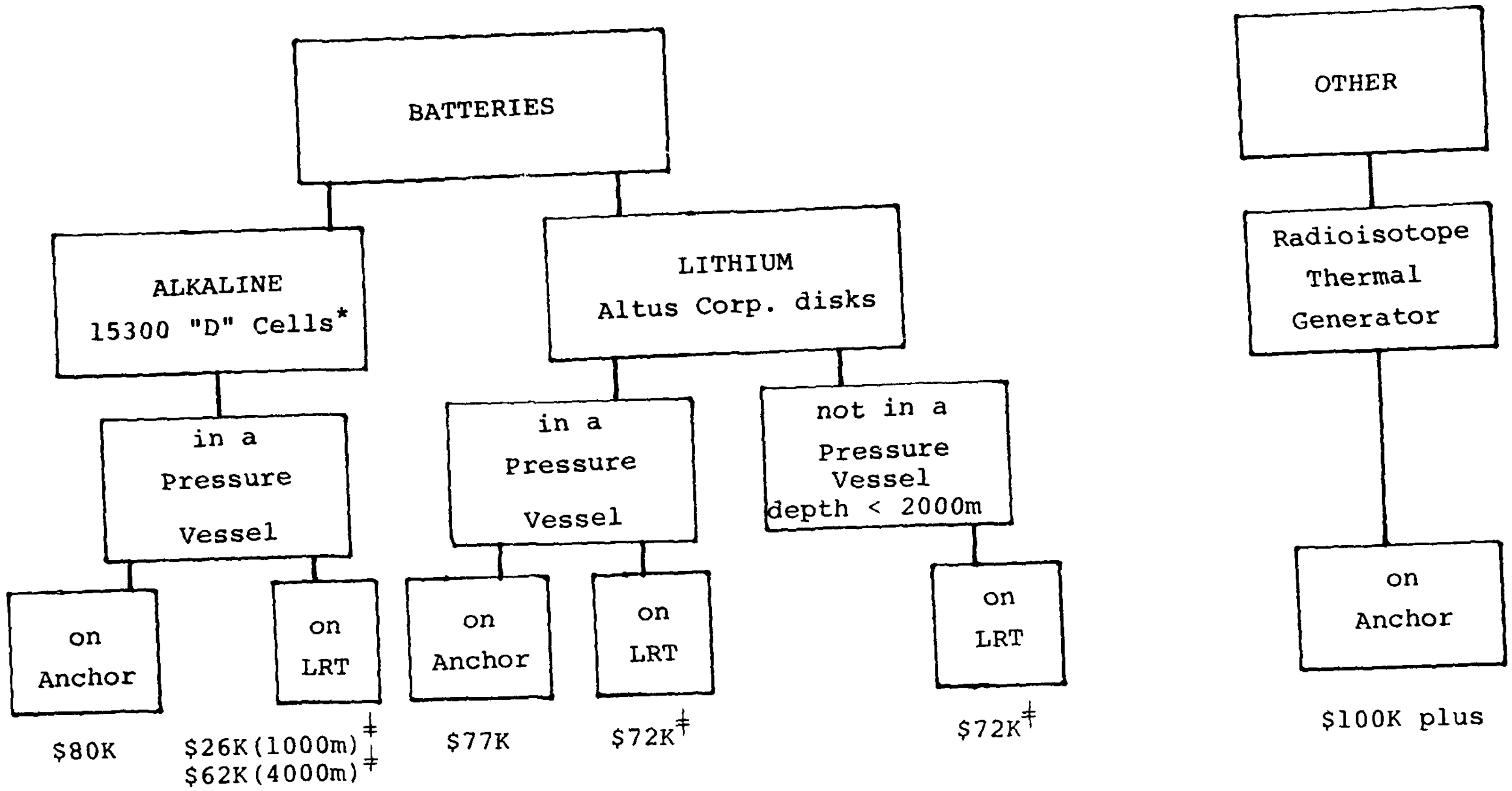

* Alkaline battery system seems impractical.

ǂ Must add cost of floatation which is considerable in case of alkaline battery.

FAMILY TREE
of
POWER SOURCES
FOR THE LONG RANGE TRANSMITTER (LRT)

Figure 4.

2) averaging would be required to take out the tidal ($\sim$ 1 m amplitude) fluctuations, 3) the procedure requires knowledge of sensor depth at zero current and 4) drift errors would be present due to creep in the mooring line or buoyancy change of the buoys.

Current Sensor

A simple calculation of current magnitude (v) required to obtain a horizontal excursion (x) gives:

$$v = \sqrt{\frac{2Bx}{\rho C_D A \ell}}$$

where B is the buoyancy (tension) in the mooring line of length ℓ, ρ is the density of seawater, C_D is the drag coefficient and A is area normal to the current direction. For B = 3000 lbs = 13344 newtons, x = 25 m, $C_D A = 100\ ft^2 = 9.29\ m^2$, $\rho = 1025.9\ kg/m^3$, v = 19 cm/sec.

Magnitude of 19 cm/sec is easily measured by a current meter. An unanswered question is whether magnitude measurement at just one location gives a reliable enough criterion for deciding the mooring's real horizontal excur- excursion. It might if averaged over the "right" period, but more study is needed.

Inclination Sensor

The average tilt of a line 2000 m long and having a horizontal excursion of 25 m is given as

$$\tan \theta = 25/2000 \approx \theta = 0.0125 \text{ radians}$$

An accelerometer measuring tilt will see a mean of 0.0125 g's, which is a good size signal. The dynamic inputs to the accelerometer would have to be either averaged or neglected and the output of the accelerometer

at zero inclination would have to be known with the desired accuracy. The most serious drawback with the tilt sensor is that it could not be placed near the top of the mooring at the LRT or receiver where the local line tilt approaches zero, regardless of the average tilt.

Tension Sensor

Resolution of 25 meters is not practical with a tension sensor. For a 2000 m long mooring with a tension (buoyancy) of 3000 lbs the change in tension due to a horizontal excursion of 25 meters is 0.23 lbs, only 1 part in 13000.

Only the current sensor seems worthy of further study.

E. Alternative Design Approaches

Various approaches were studied to meet the performance goals of the tomography moored array design. For each specific design approach strawman source and receiver mooring designs were outlined. Distributed buoyancy, discrete line tapering and accommodation of the full range of desirable source and receiver depths were considered as subvariations within each strawman.

The first approach and the main focus of our design studies is outlined below.

Approach A

- Separate source and receiver moorings.
- Stiff source and receiver moorings.
- A separate satellite telemetry mooring placed alongside each receiver mooring. Intercommunication between the Receiver/Processor (RP) and the Pop-Up-Buoy (PUB) is accomplished by means of a two-way acoustic telemetry link. The PUB is a satellite communication buoy which rests safely nested atop a subsurface moored buoy except during brief periods every few days when it surfaces to transmit data. It is described in DAHLEN, et al. (1981).
- Ship-to-Long Range Transmitter (LRT), Ship-to-RP and Ship-to-PUB two-way acoustic telemetry links are provided.
- Alarm sensors located on source and receiver moorings.
- PUB can transmit but not receive RF.

Source Moorings(s)

- Alarm can be sounded only by omitting part or all of the transmission sequence.
- One alarm sensor (most probably a simple current magnitude sensor) mounted on LRT.
- LRT depth 1000 m to 4000 m.
- Ocean bottom is 5000 m.
- High-power/low-drift clock can only be interrogated via the Ship-to-LRT acoustic link.
- Acoustic Release is located in the LRT.

Configurations

1. Top buoyancy provided by a syntactic foam sphere.
   - LRT and the top buoyancy at the same depth.
   - Lithium primary battery placed with LRT.
   - Tension member is 3 x 19 USS wire rope (jacketed).
2. Same as 1. except:
   - Top buoyancy provided by steel sphere.
3. Same as 2. except:
   - Steel sphere above LRT (at much less pressure).
4. Same as 1. except:
   - Lithium primary battery placed upon the anchor.
   - Electromechanical cable (also the tension member) connects the battery with the LRT.
5. Same as 4. except:
   - Top buoyancy provided by steel sphere.
6. Same as 5. except:
   - Steel sphere above LRT at much less pressure.

7. Same as 1. except:
   - Top buoyancy provided by faired glass balls.

8. Same as 4. except:
   - Top buoyancy provided by faired glass balls.

Receiver Mooring (R)

- RP depth is 1000 m ~ 3500 m.
- Ocean depth is 5000 m.
- One alarm sensor (most probably a simple current magnitude sensor) mounted in RP.
- RP contains its own power source.
- Dead-weight anchor.
- Acoustic Release is located in the RP.

Configurations

1. - Top buoyancy provided by a syntactic foam sphere.
   - 3 x 19 USS wire rope (jacketed) used as the tension member.
   - RP and the top buoyancy at the same depth.

2. Same as 1. except:
   - Top buoyancy provided by steel sphere.

3. Same as 2. except:
   - Steel sphere (top buoyancy) is above RP.

4. Same as 1. except:
   - Top buoyancy provided by faired glass balls.

Satellite Telemetry Mooring (T)

- Ocean depth is 5000 m.
- Top subsurface float depth is 45 m.
- Top subsurface float is a steel sphere.

- USS 3 x 19 jacketed wire rope is used as the tension member.
- Anchor is dead-weight.
- Acoustic Release is located under the lowest floatation.
- PUB is a 22" ϕ sphere. A winch is located in the PUB and a 5/32" ϕ wire (O.D. 3/16") is used as the tether between the PUB and the top subsurface float.

Configurations

1. All buoyancy (exclusive of PUB) is provided at the 45 m depth.

2. Buoyancy is provided at two depths. One at 45 m and the other deeper.

Alternative approaches considered but not studied in detail include:

Approach B

- Separate source and receiver moorings
- Stiff source moorings
- Combined receiver/satellite telemetry moorings. Intercommunication is accomplished by either a two-way acoustic telemetry link or hardwire.
- Excursion tracking of receiver/satellite telemetry mooring.
- Ship-to-LRT and ship-to-RP two-way acoustic telemetry links are provided.
- Alarm sensor located on source mooring.

Source Moorings(s)

- Alarm can be sounded only by omitting part or all of the transmission sequence.
- One alarm sensor (most probably a simple current magnitude sensor) mounted on LRT.
- LRT depth 1000 m to 4000 m.
- Ocean bottom is 5000 m.
- High-power/low-drift clock can only be interrogated via the Ship-to-LRT acoustic link.
- Acoustic Release is located in the LRT.

Receiver/Satellite Telemetry Moorings (RT)

- Receiver depth 1000 - 3500 m.
- Ocean depth is 5000 m.
- Receiver contains its own power source.
- Dead weight anchor.
- Pop-Up-Buoy is nested atop subsurface float at 45 m. It talks directly with the receiver module (acoustic or hardwired) or to a ship. It can transmit but not receive RF.
- Subsurface float is a steel sphere.

Approach C

- Combined source/receiver moorings.
- Stiff source/receiver moorings.
- A separate satellite telemetry mooring implanted alongside each receiver mooring. Intercommunication is accomplished by means of a two-way acoustic telemetry link.
- Ship-to-LRT/RP two-way acoustic telemetry link is provided.
- Alarm sensor located on source/receiver mooring.

Source/Receiver Mooring (SR)

- Top depth (Transmitter depth) 1000 m - 4000 m
- Receiver depth 1000 m - 3500 m
- Ocean depth is 5000 m.
- One alarm sensor (unspecified)

Satellite Telemetry Mooring (T)

- (Same as Approach A)

Approach D

- Combined source/receiver/satellite telemetry moorings. Intercommunication is accomplished by either a two-way acoustic telemetry link or hardwired.
- Excursion tracking of source/receiver/satellite telemetry moorings.
- Ship-to-LRT/RP/PUB acoustic telemetry link is provided.

Source/Receiver/Satellite Telemetry Moorings (SRT)

- Source depth 1000 m - 4000 m.
- Receiver depth 1000 m - 3500 m.
- Ocean depth 5000 m.
- Pop-UP-Buoy is nested atop subsurface float at 45 m. It talks directly with the receiver module (or a ship). It can transmit but not receive RF.
- Subsurface float is a steel sphere.

III. ANALYSIS

This section presents results from computer simulations of mooring excursions for single-point moorings. The cost of each mooring is calculated and plotted against excursion, mooring length and mooring type. Approach A as outlined in section II is the focus of this analysis. The cost of other approaches can be derived from the cost of approach A.

A. Design Assumptions

1. Wire and Rope a) U.S. Steel 3 x 19 polyethylene jacketed "Oceanographic Wire Rope" of constant diameter. This wire rope has become the "standard" for oceanographic moorings. Although we have not considered alternatives to USS 3 x 19 wire, much money might be saved by switching to a more competitively marketed "non-rotating" wire. Of course, the ocean qualification testing *such wire would* require is rather daunting. b) Industry-standard polyethelene jacketed, single conductor, electromechanical armored cable. This cable is not precisely torque-balanced but has been used successfully on moorings. c) Safety factor of 2 for both the wire rope and the EM cable. For USS 3 x 19 wire rope used for subsurface moorings a safety factor of 2 has proven satisfactory in recent deployments. d) Line normal drag coefficient of 1.4 (for flow component normal to the line) and line skin friction drag coefficient of 0.01 (for flow component parallel to the line).

Kevlar as a mooring line tension member was ruled out for the following reason:

For a given working load, Kevlar and 3 x 19 USS wire rope cost about the same but Kevlar has a larger diameter.

Larger diameter means larger mooring excursions. On the other hand, for a given mooring excursion, Kevlar mooring line has a larger working load. A larger working load requires more buoyancy and even larger diameter rope. These make the Kevlar mooring significantly more expensive than the wire mooring.

In comparing Kevlar with wire rope different safety factors (breaking strength divided by working load) were assumed. One manufacturer (Wall Rope Works) of Kevlar recommends working loads for non-critical applications to be figured at 20% to 25% of average breaking strength. This compares unfavorably with the 50% used for 3 x 19 USS wire ropes in recent deployments. For a given large (greater than 2000 lbs) working load, Kevlar (safety factor - 4) requires a larger diameter than wire rope (safety factor = 2). Larger diameter gives proportionally larger drag and larger drag means much larger mooring excursion, greater than proportionally.

For a 5000 lbs working load a suitable Kevlar rope (1/2", average breaking strength 22,000 lbs) costs $1.21/foot (1982 prices). A comparable 3 x 19 USS wire rope (5/16", breaking strength 10,300 lbs) costs $1.02/foot (1982 prices). But because the wire rope weighs 0.097 lbs/ft more in water (0.125 lbs/foot versus 0.028 lbs/foot), it requires more floatation at an added cost of $0.43/foot (recent price of $4.40/lb) to obtain the same average tension in the wire rope mooring. Hence, the effective cost of wire rope is $1.45/foot compared to Kevlar's $1.21/foot. This difference was insignificant when comparing costs of the two mooring systems.

Fairings were not included because of very high cost, deployment difficulty, and sometimes questionable effectiveness in small currents.

2. <u>Buoyancy</u> a) Spherical top float. The float is either syntactic foam or steel. Steel spheres are either models marketed by ORE or are our own hypothetical designs (see Appendix D). Drag coefficient used for these spheres is 0.05. b) Glass balls in clusters of four. Each cluster is packed in a commercially available fairing which has a drag coefficient multiplied by area of 3.2 ft^2.

In general, excursions can be reduced by 10-20% if extra buoyancy is allowed to be distributed along the wire, because a higher average tension is possible.

3. <u>Instrumentation</u> a) Receiver/Processor package. This is an 8-inch diameter, 6 foot long cylinder and weighs 300 pounds dry and 150 pounds wet. It includes its own battery. b) Long-Range Transmitter. The package has three cylinders: 1 of 1-foot diameter, 20 feet long, flanked by 2 of 1-foot diameter, 14 feet long. It weighs 1500 lbs dry and 500 lbs wet. Another cylinder houses the lithium battery power source for the LRT. Depending upon working depth (1000 - 5000 m) its diameter is 19-25 inches, its length is 45-47 inches, its weight is 760 - 2620 lbs dry and 360 - 1980 lbs wet. It is located at either the LRT or the anchor. See Appendices B and C.

Detailed specifications and costs of the mooring lines, buoyancy, instruments and anchors used in this study are listed in the tables of mooring component characteristics in Appendix C.

B. Results

On the following pages are plots of cost versus excursion and cost versus depth, for various mooring types. These are given independently for source and receiver moorings, and for the two current profiles described in section II. B. The plots represent the result of hundreds of runs of computer program DYNOSUB.

Of particular interest are the plots of cost versus depth, with the horizontal excursions of the transmitter and the receiver held constant at 25 meters. These plots provide, in summary form, a direct comparison of competing mooring configurations. A full description of each configuration is given above in section II. E.; curves on the plots below are keyed to these by a code signifying Approach: Instrument: Configuration. For example, "AR3" denotes a Receiver mooring using approach A, configuration 3.

Our computer runs and plots explicitly consider only approach A; that is, separate source and receiver and telemetry moorings, without excursion monitoring. However, costs of moorings using other approaches can be inferred. For instance, the cost of an excursion-tracked mooring is simply the cost of tracking equipment plus the cost of a large-excursion, soft mooring (given on the cost versus excursion plots). The cost of a combined source and receiver mooring is the cost of a source mooring plus that of the buoyancy needed to support the receiver/processor instrument (because the drag added is relatively small).

C. Conclusions and Observations

1. Most of the drag is provided by the line, not the buoys or instruments. Therefore the thickness of the line's jacket should be minimized. Excursion will be very sensitive to this, and relatively insensitive to the size or weight of the instruments and buoys.

2. The curves of cost versus excursion are almost hyperbolic; cost is insensitive to excursion when excursions are high, but excursion is very insensitive to cost when excursions are low. For example, for profile 2, all excursions over 40-60 meters are cheap, while excursions under 20-30 meters become astronomically expensive.

3. Buoyancy materials: glass balls are the cheapest for deep sources and receivers, while shallow steel spheres (about 450 m. depth) are cheapest for less-deep instruments. A deeper steel sphere (about 1000 m. depth) is too expensive. Syntactic foam is also more expensive, but may be preferable to glass balls for intermediate depths, because of the large number of balls required. For example, a source mooring to have 27 meters excursion under profile 2 at 2000 meters uses 240 17-in glass balls!

4. Electromagnetic cable between the LRT and its power source on the anchor appears to be the most economical approach for LRTs deeper than about 1500 meters. However, this cost advantage diminishes and may reverse if plain wire is used (wire that's not premium priced as is USS 3 x 19).

5. The bottom line: How much does a stiff tomographic mooring cost? Assuming 25 meters horizontal excursion under profile 2, the answer, with minimum cost configurations, is:

Instrument Depth (meters)	Receiver mooring without receiver/processor (1000 $)	Source mooring without LRT, but with battery* (1000 $)
1000	108	184
1500	95	160
2000	60	136
2500	39	114
3000	25	92
3500	16	87
4000	10	81

* includes LRT power supply for $72,000.
Note that the receiver moorings cost about the same as source moorings minus the LRT power supply.

6. Comparing the effects of profile 1 with those of profile 2 shows that excursions and costs are very sensitive to the current profile. Therefore, for any deployment site, it's vital to have a good prediction of the particular currents there, so that a suitably stiff mooring can be chosen. For currents much greater than profile 2, moorings with less than 25 meters horizontal excursion are essentially impractical unless the instruments are deep.

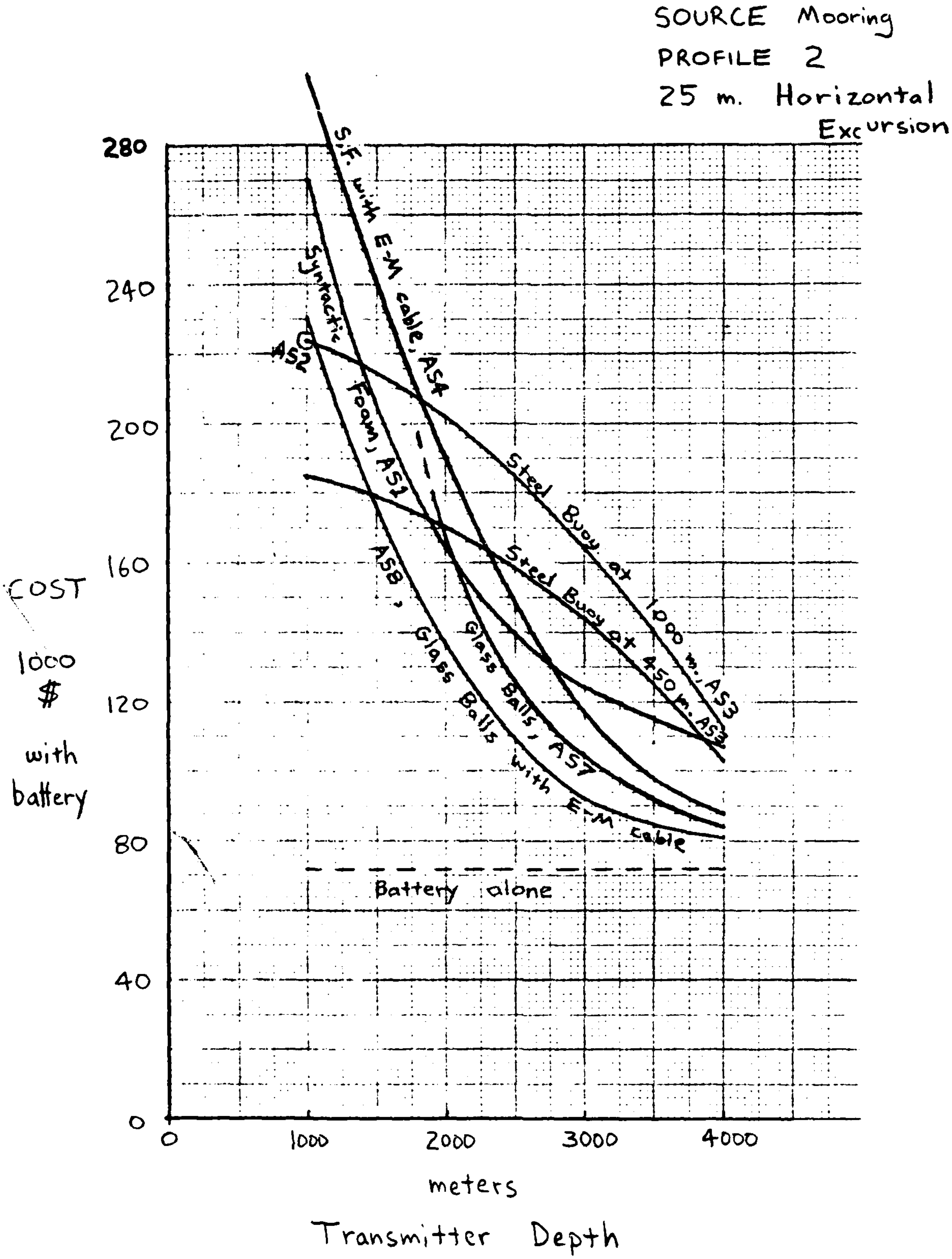

FIGURE 4

Cost comparison of mooring configurations for the Long Range Transmitter (LRT), as a function of LRT depth, for a particular current profile and horizontal excursion.

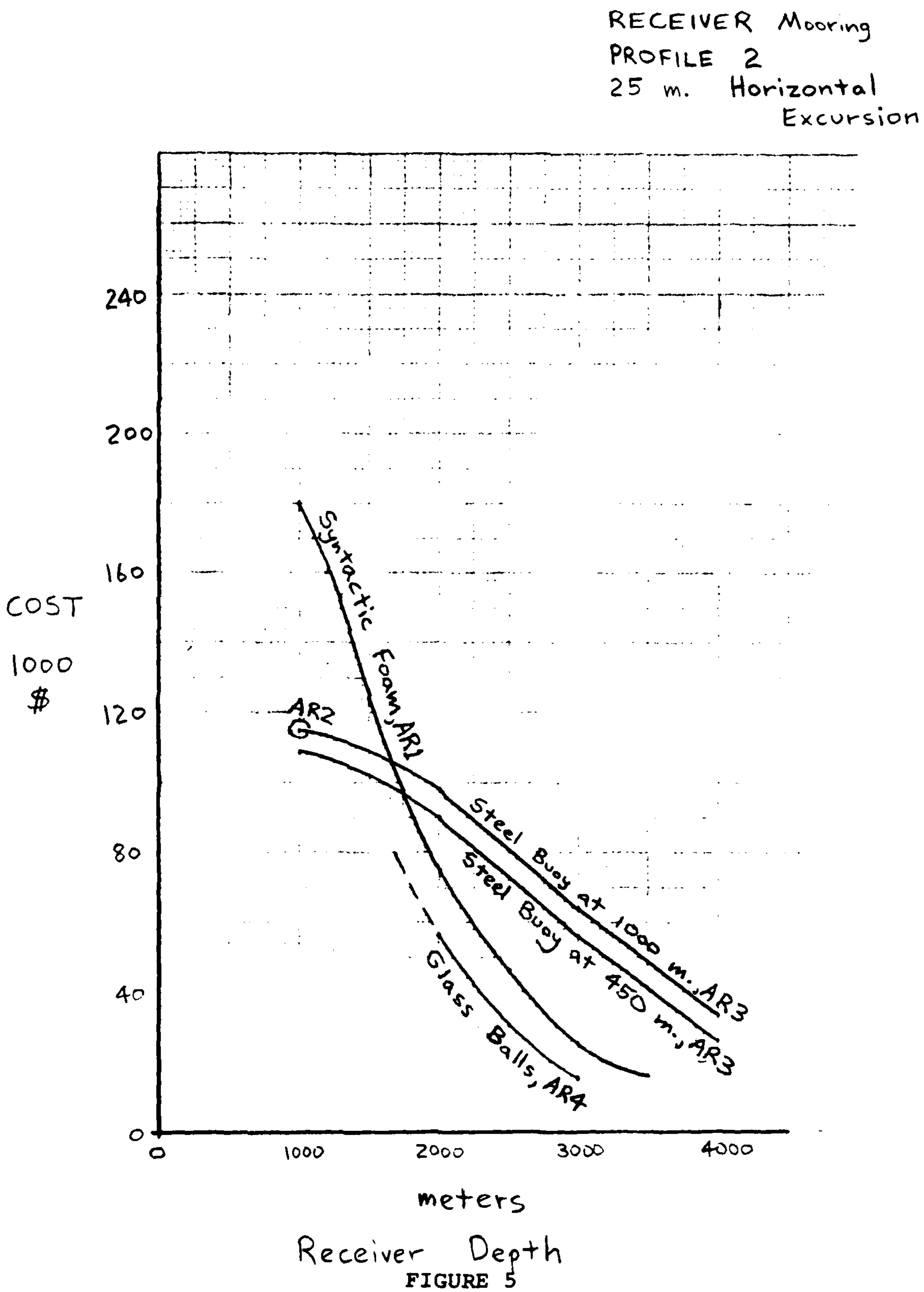

FIGURE 5

Cost comparison of mooring configurations for the acoustic Receiver, as a function of receiver depth, for a particular current profile and horizontal excursion.

SOURCE mooring
PROFILE 2
LEAST COST
CONFIGURATIONS

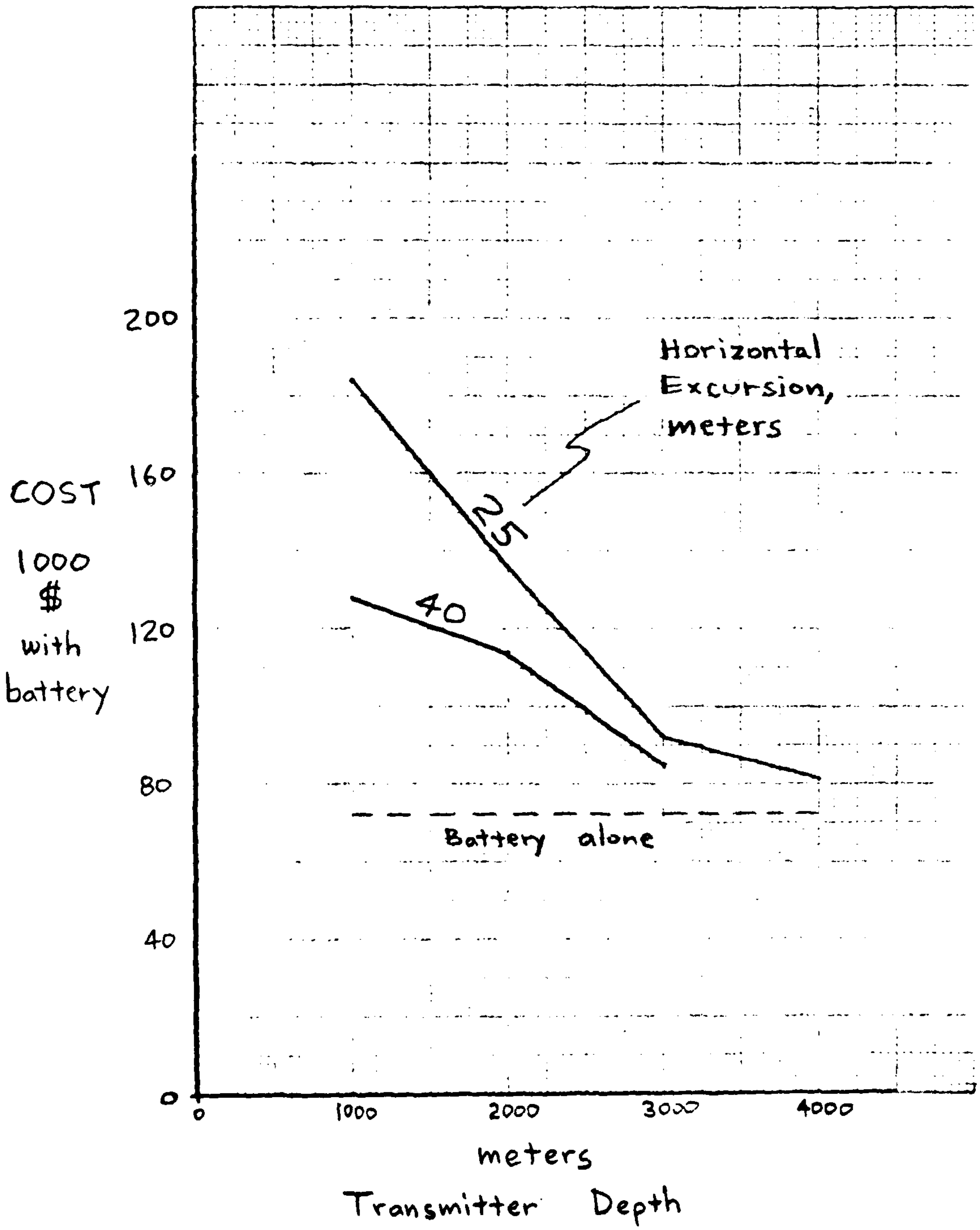

FIGURE 6
Minimum LRT mooring cost, as a function of LRT depth and horizontal excursion.

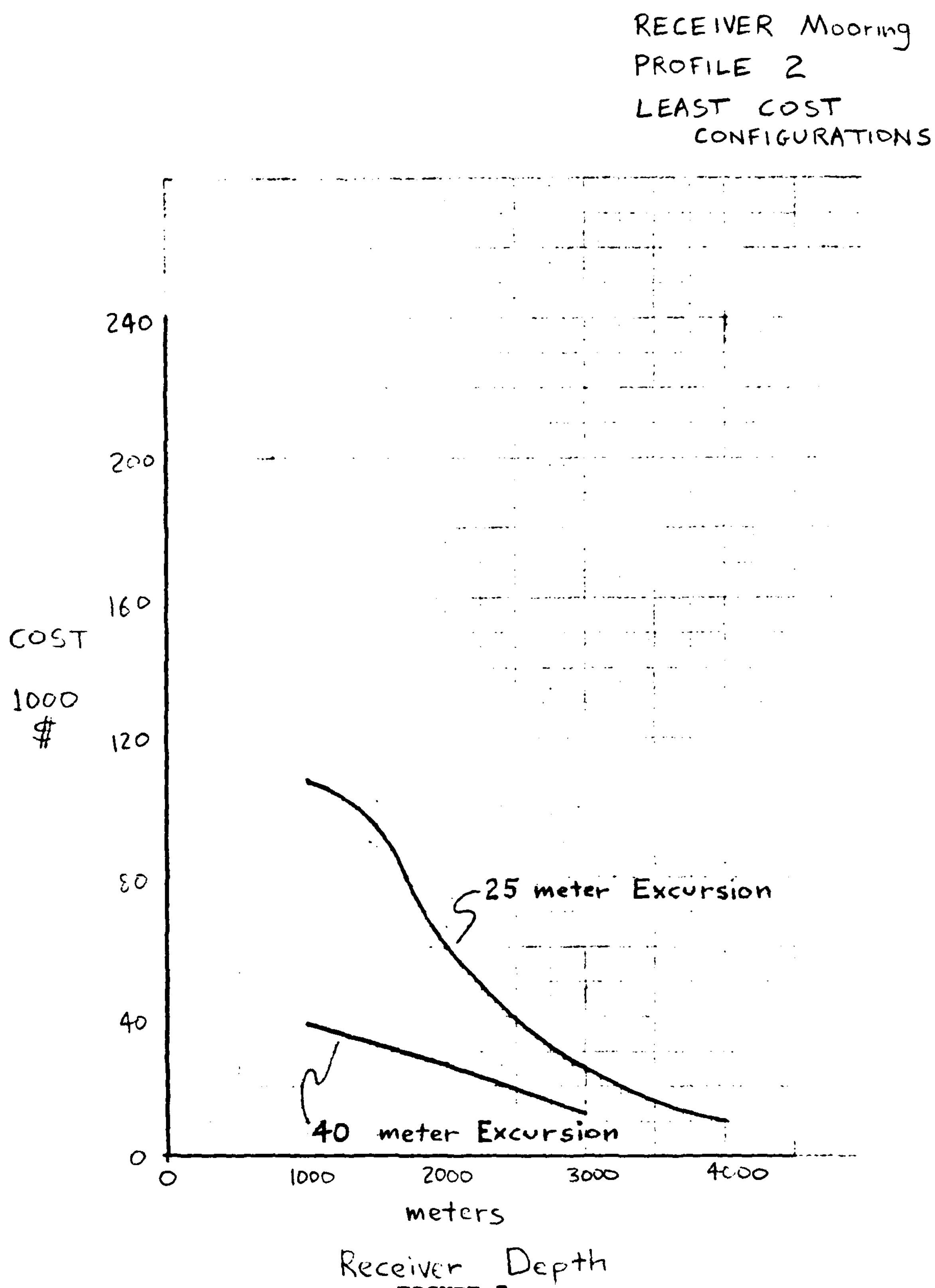

FIGURE 7

Minimum Receiver mooring cost, as a function of Receiver depth and horizontal excursion.

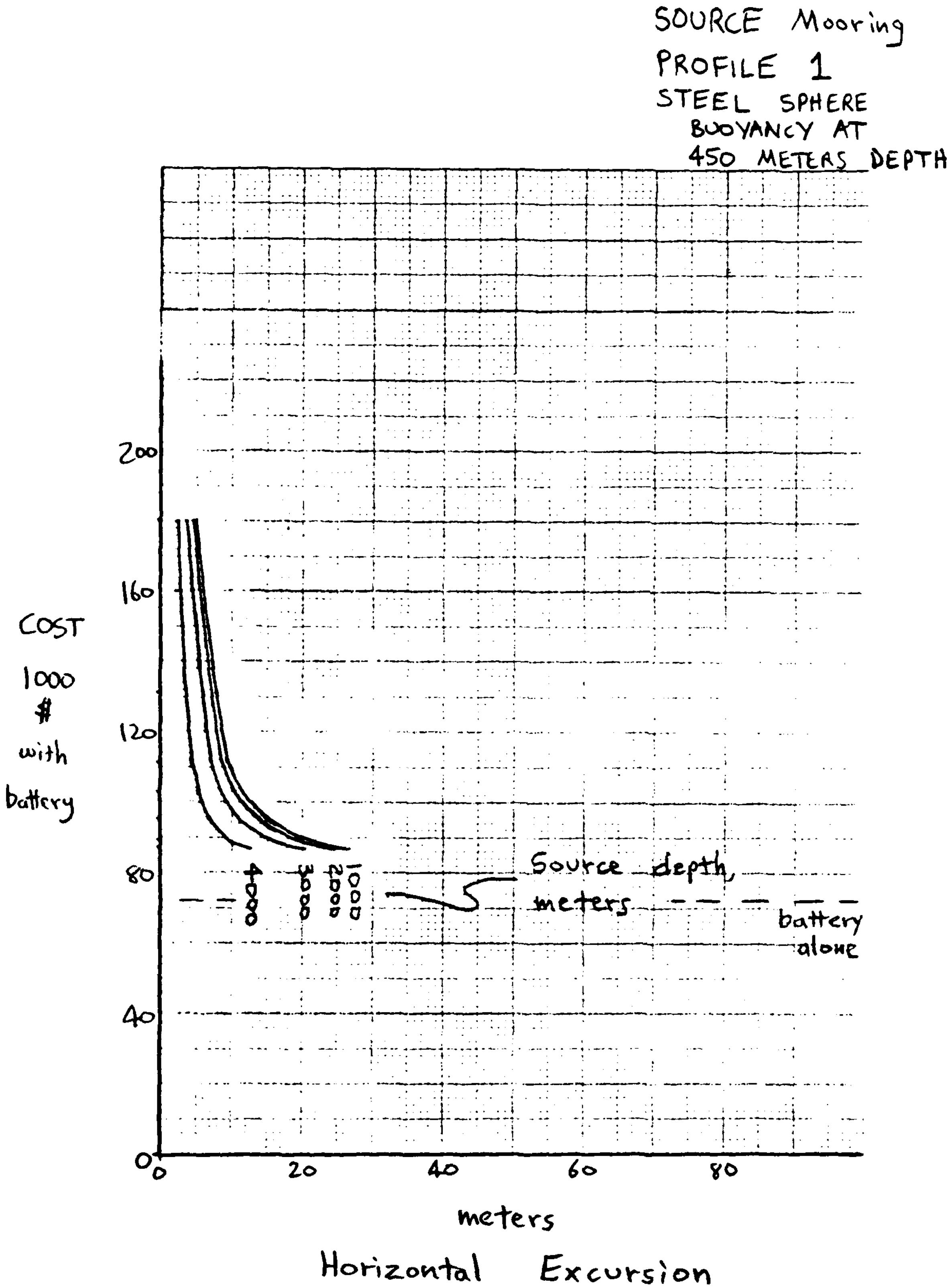

FIGURE 8

Cost vs. excursion, depth for mooring design AS3 under current profile 1.

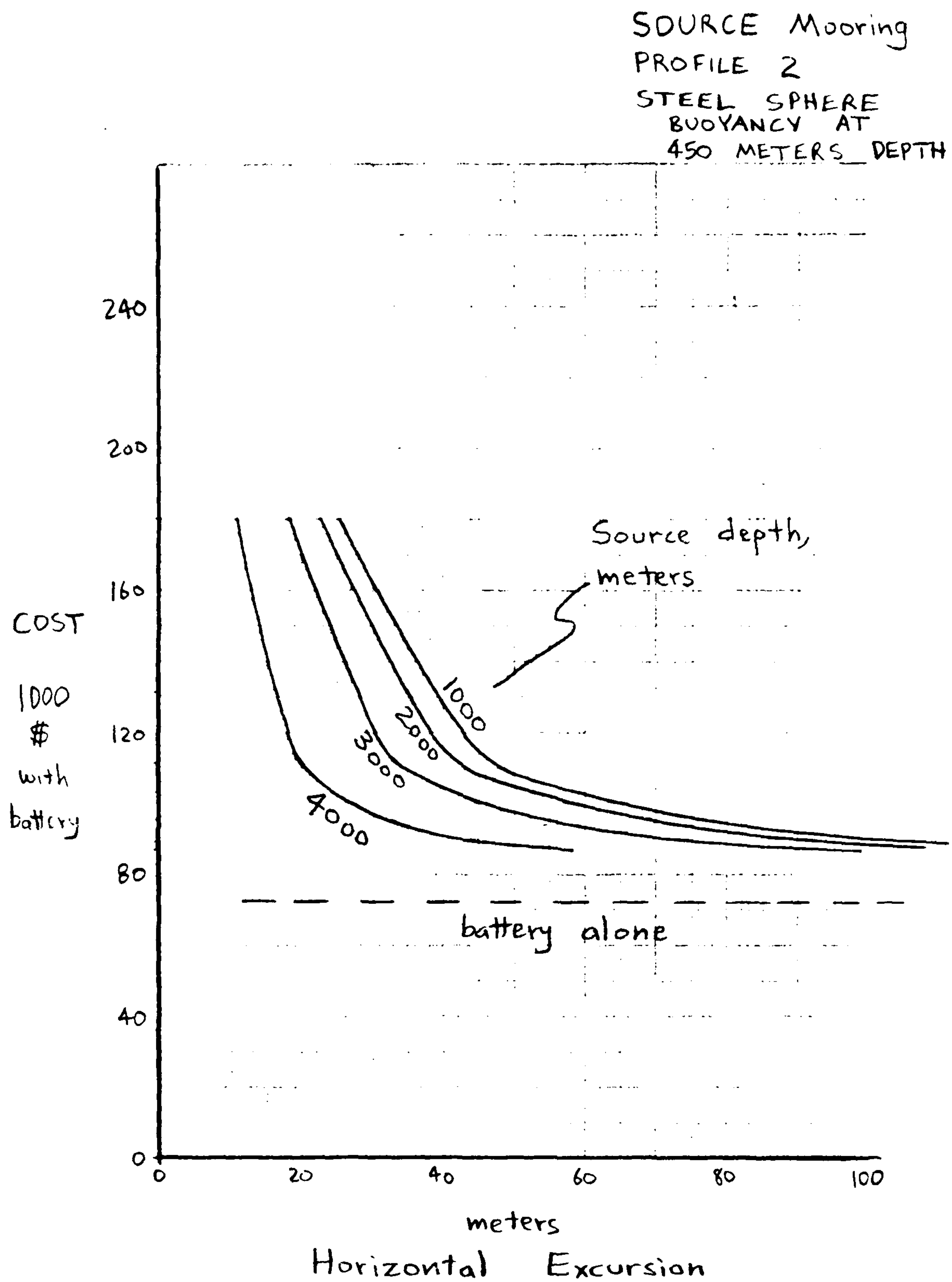

FIGURE 9

Cost vs. excursion, depth for mooring design AS3 under current profile 2.

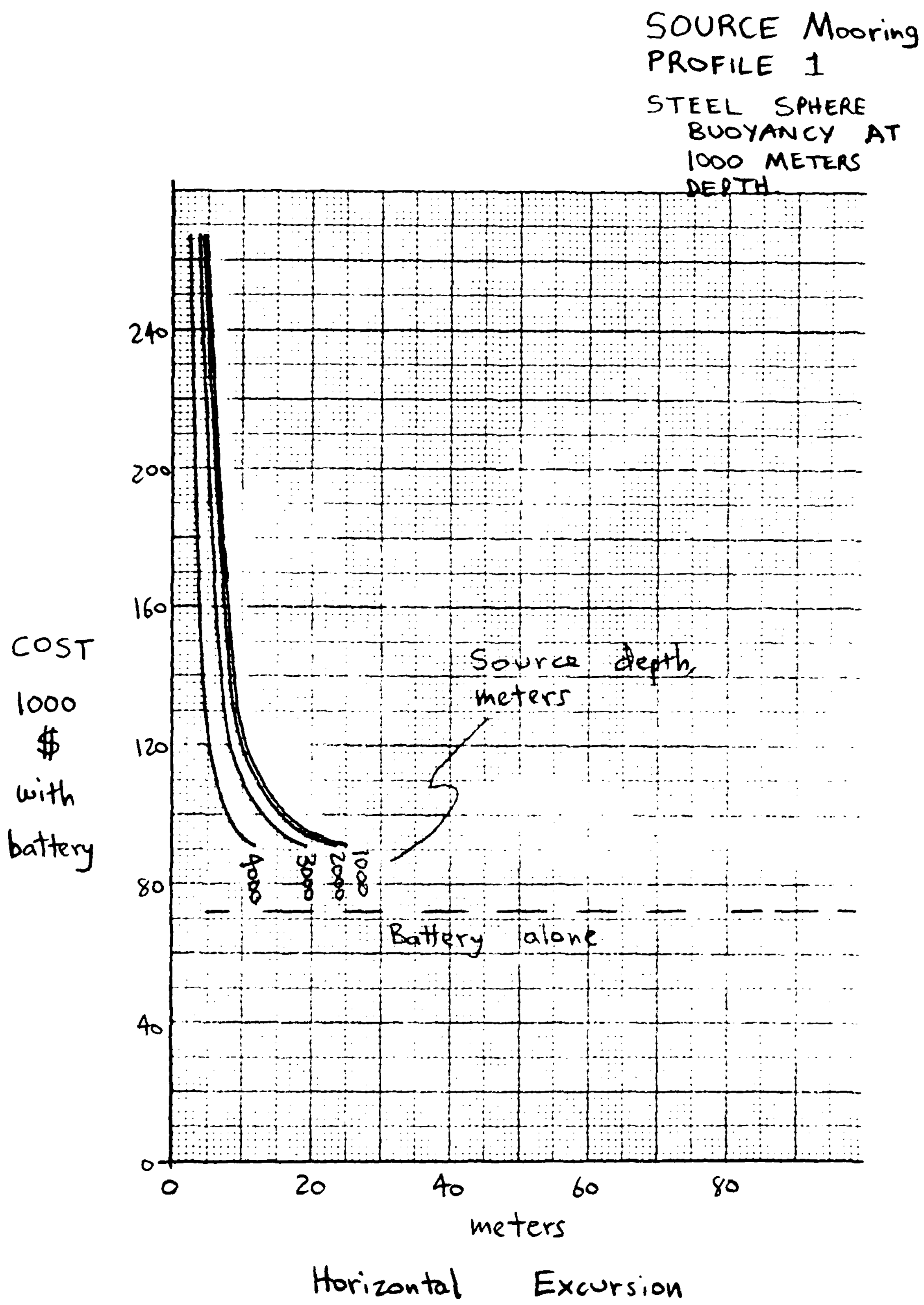

FIGURE 10

Cost vs. excursion, depth for mooring designs AS2 and AS3 under current profile 1.

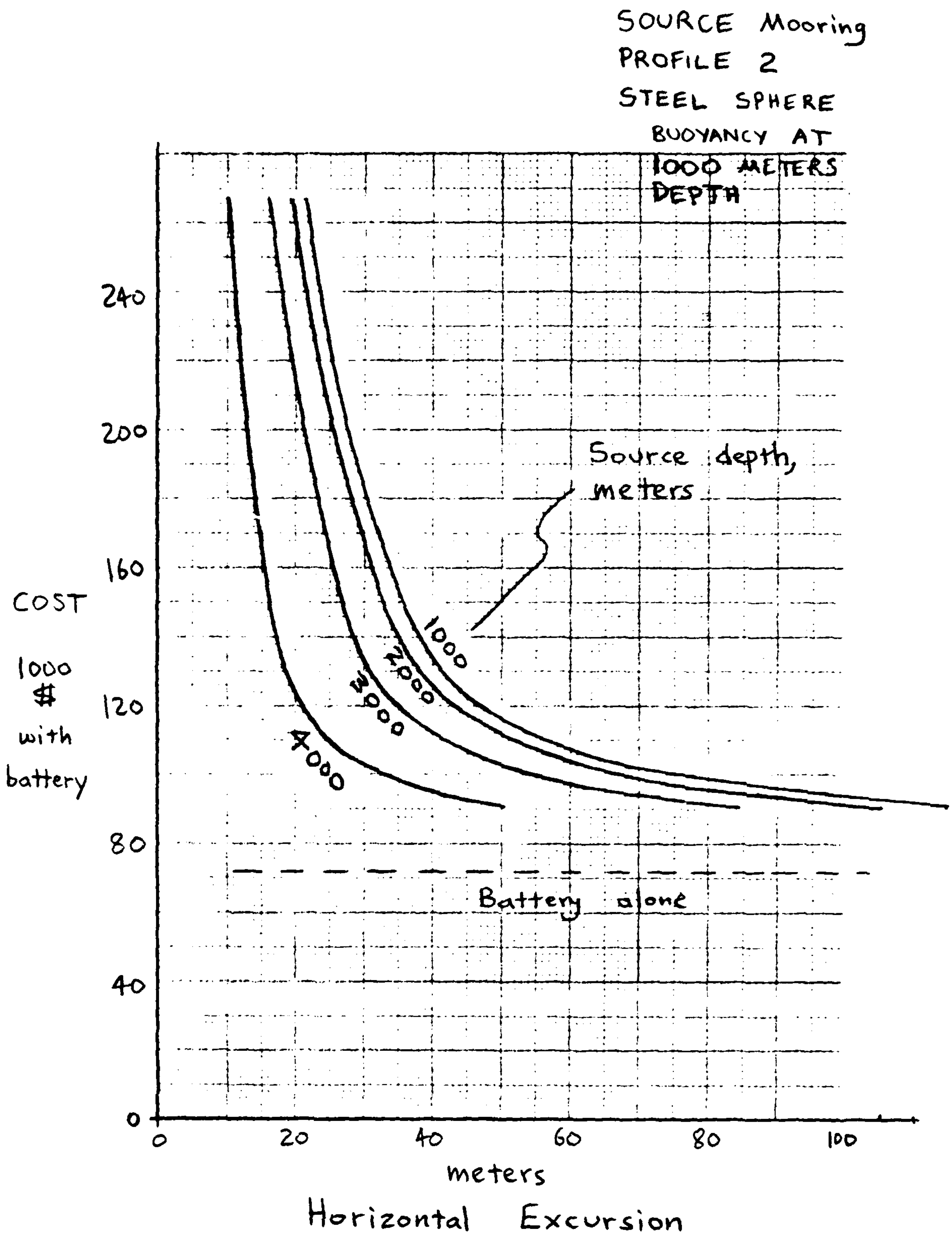

FIGURE 11

Cost vs. excursion, depth for mooring designs AS2 and AS3 under current profile 2.

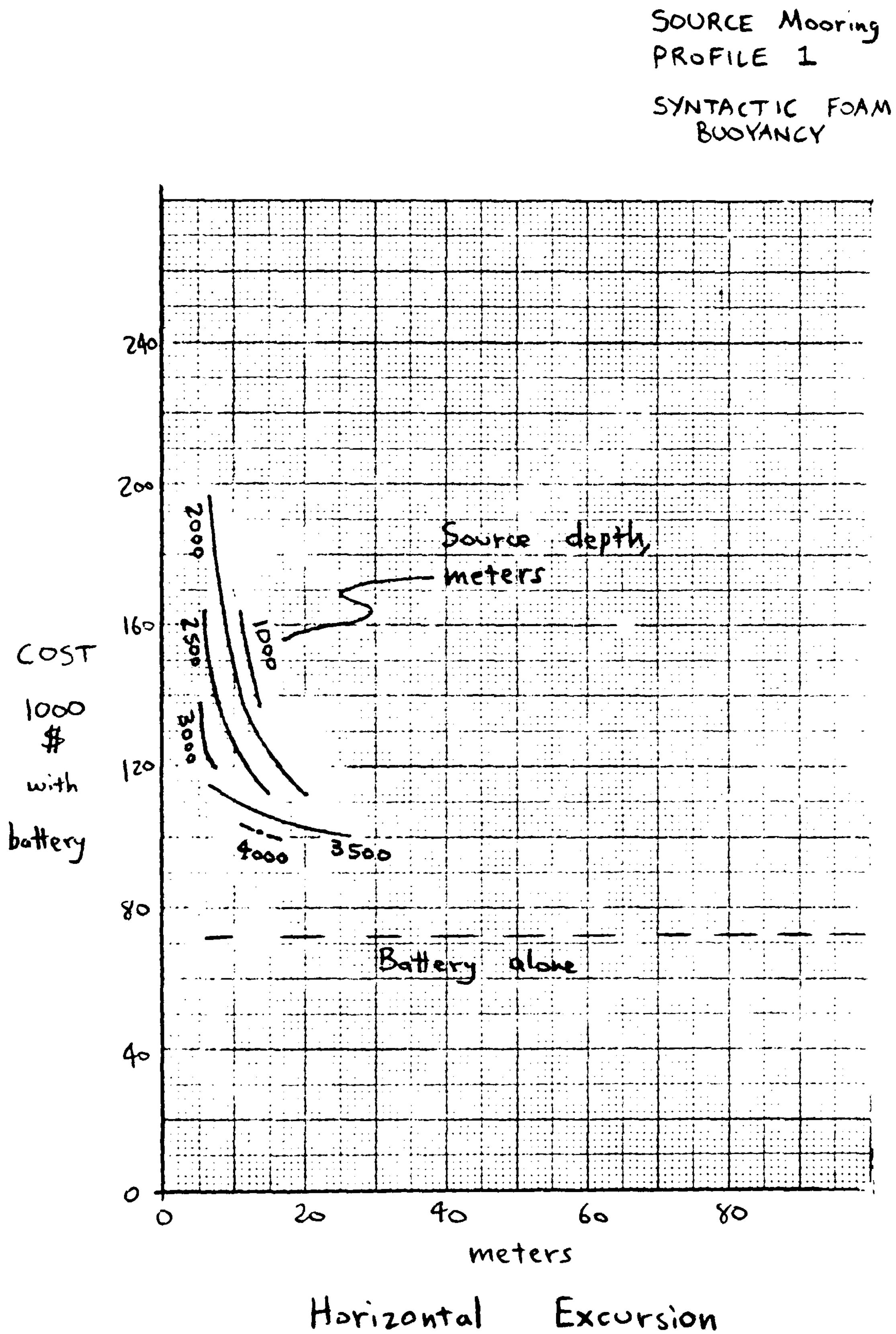

FIGURE 12

Cost vs. excursion, depth for mooring design AS1 under current profile 1.

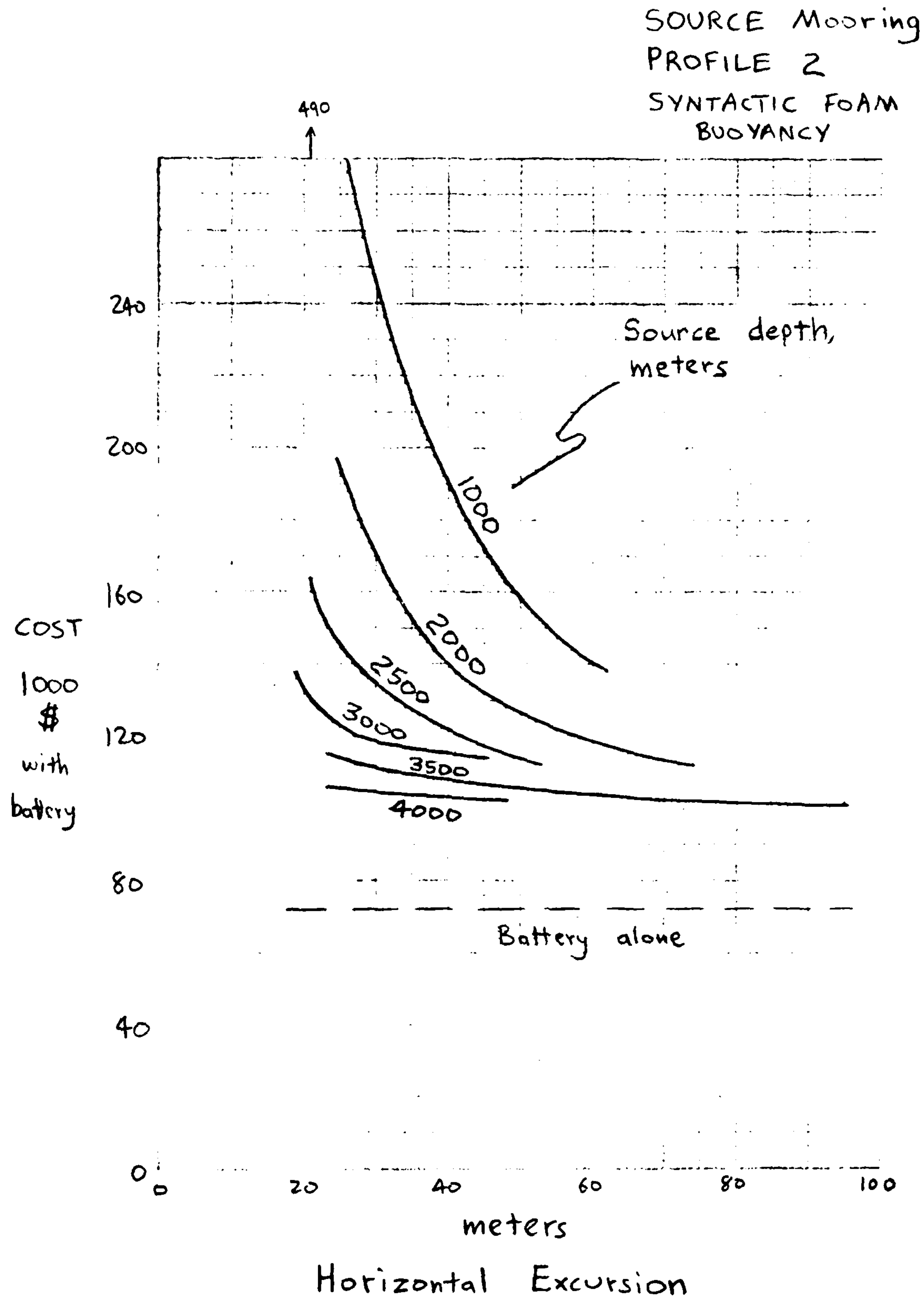

FIGURE 13

Cost vs. excursion, depth for mooring design AS1 under current profile 2.

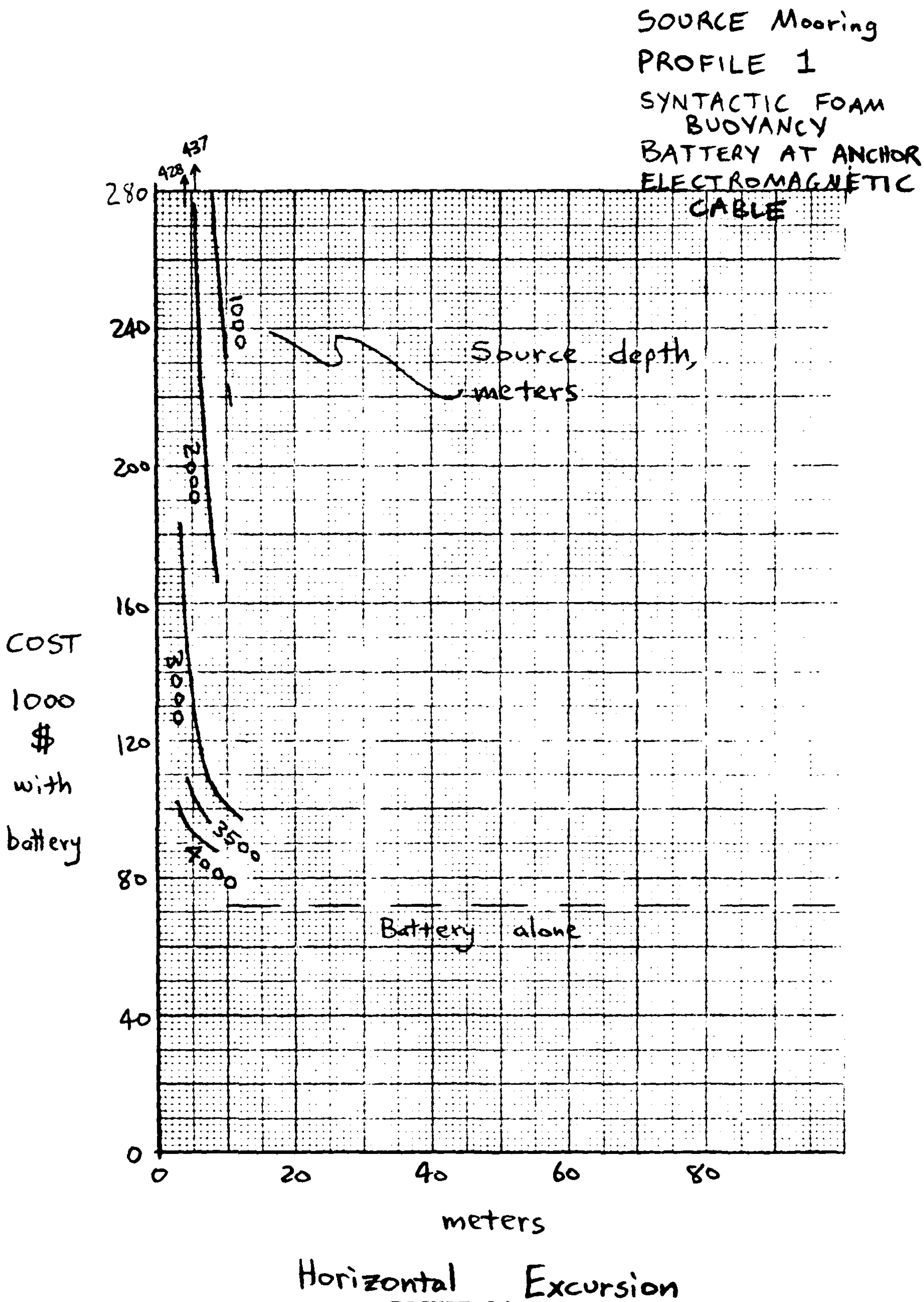

FIGURE 14
Cost vs. excursion, depth for mooring design AS4 under current profile 1.

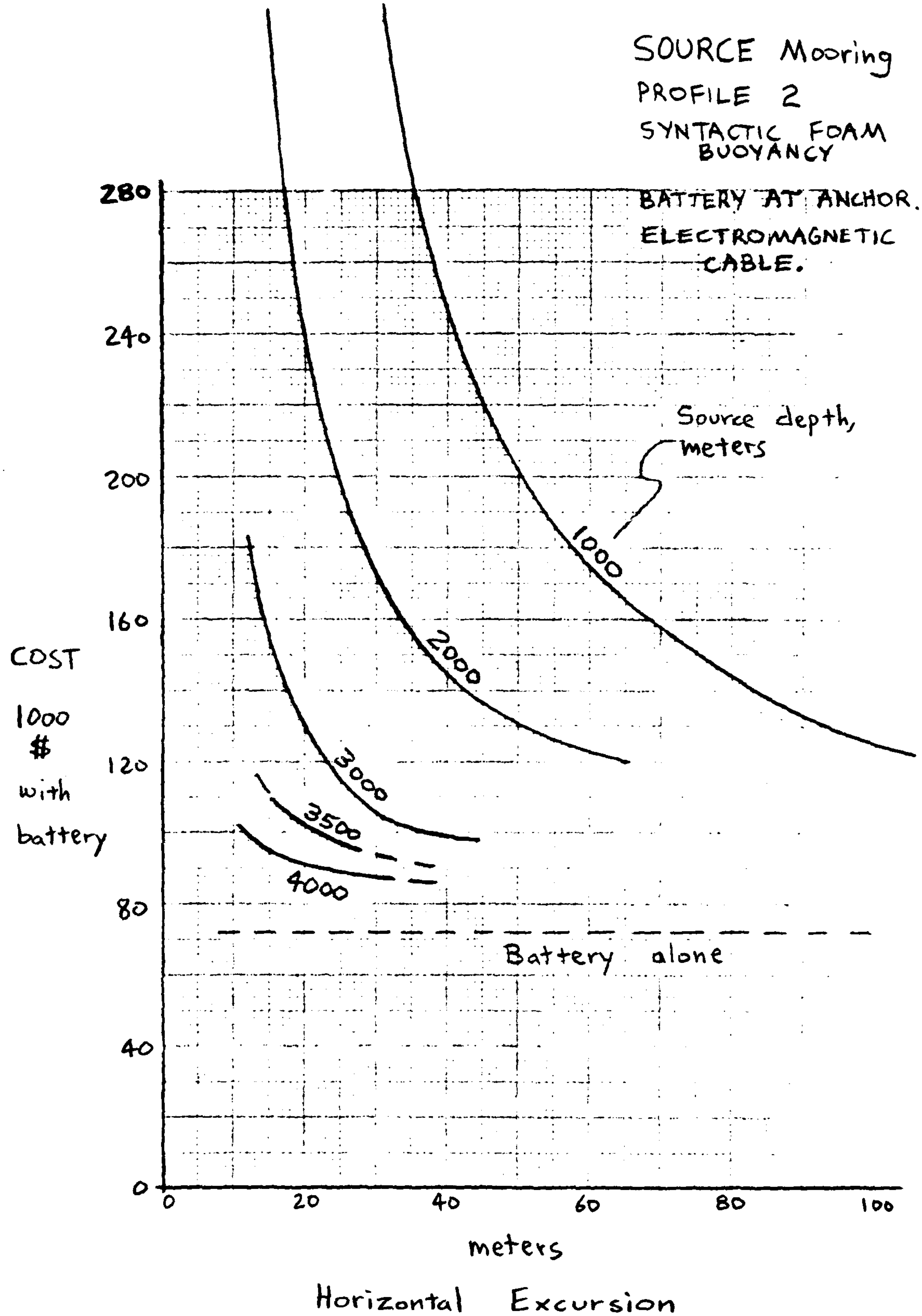

FIGURE 15

Cost vs. excursion, depth for mooring design AS4 under current profile 2.

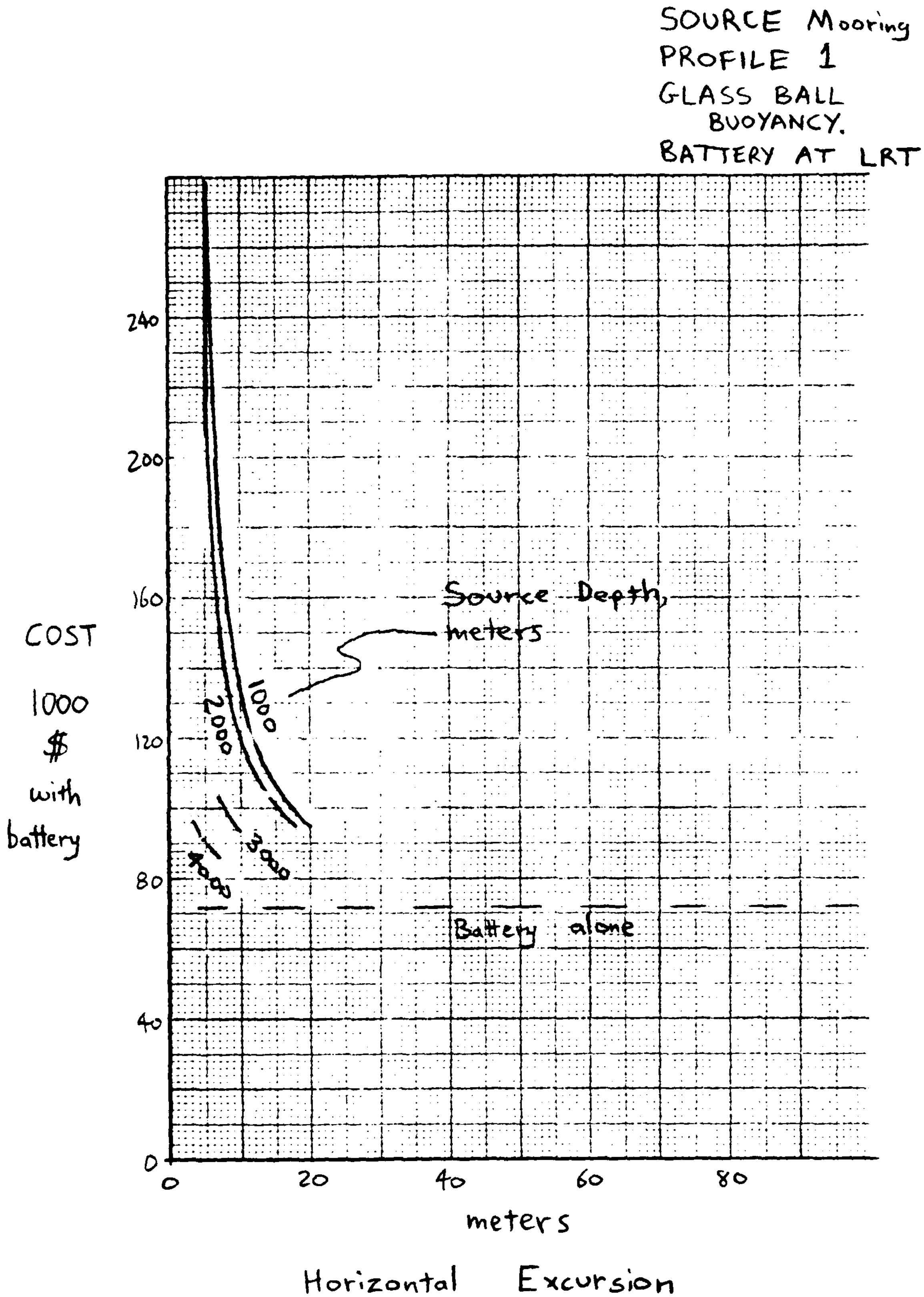

FIGURE 16

Cost vs. excursion, depth for mooring design AS7 under current profile 1.

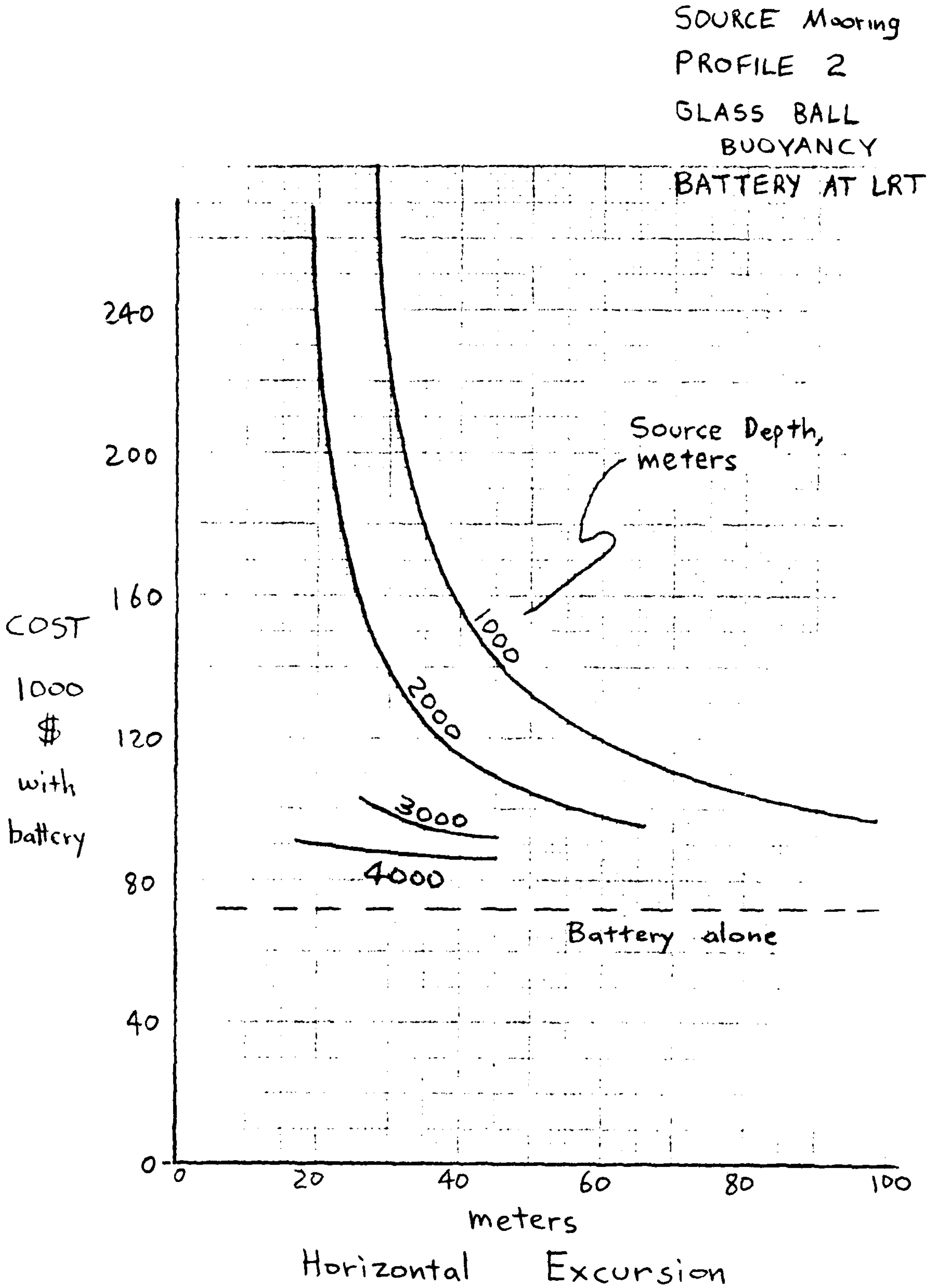

FIGURE 17

Cost vs. excursion, depth for mooring design AS7 under current profile 2.

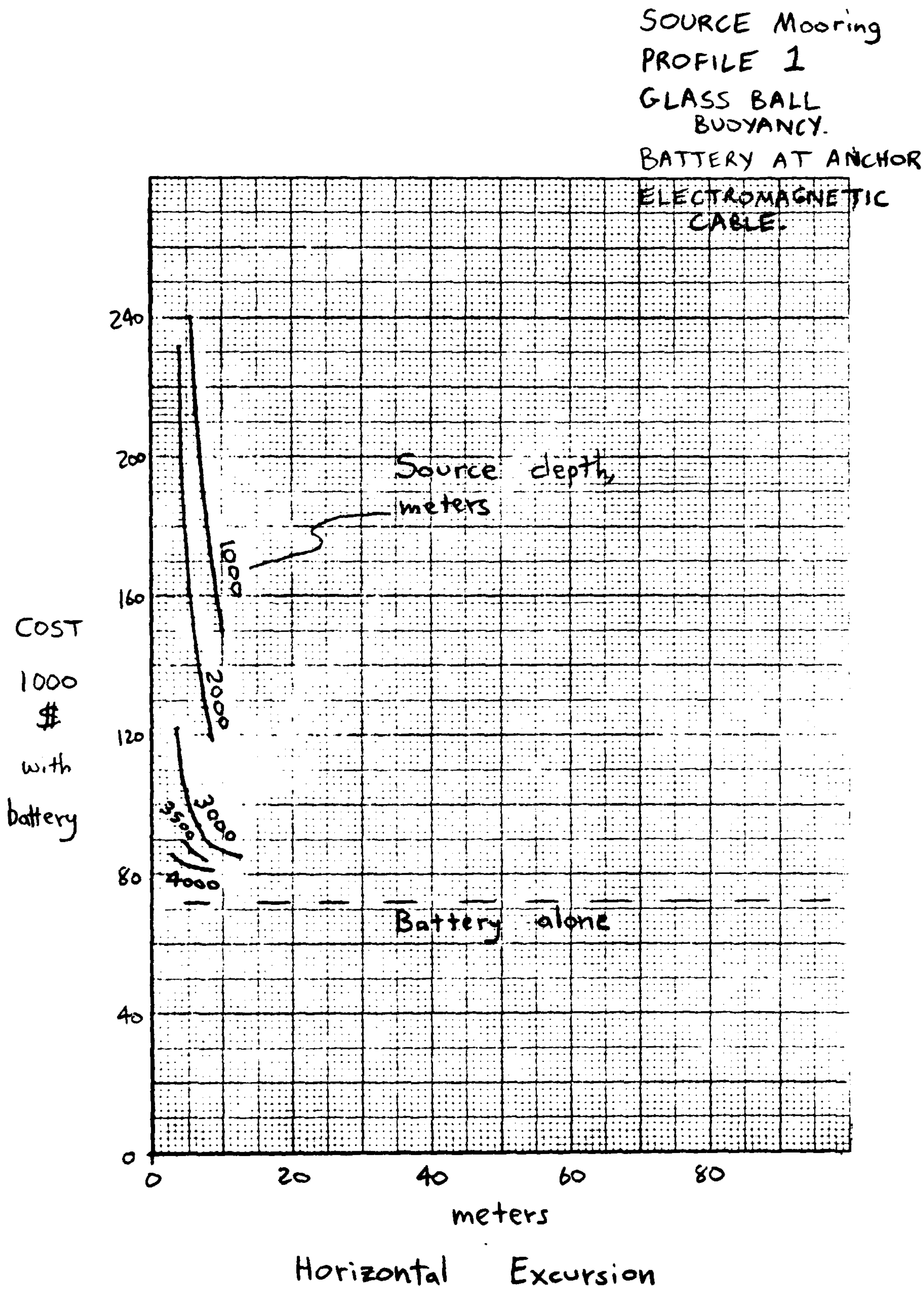

FIGURE 18

Cost vs. excursion, depth for mooring design AS8 under current profile 1.

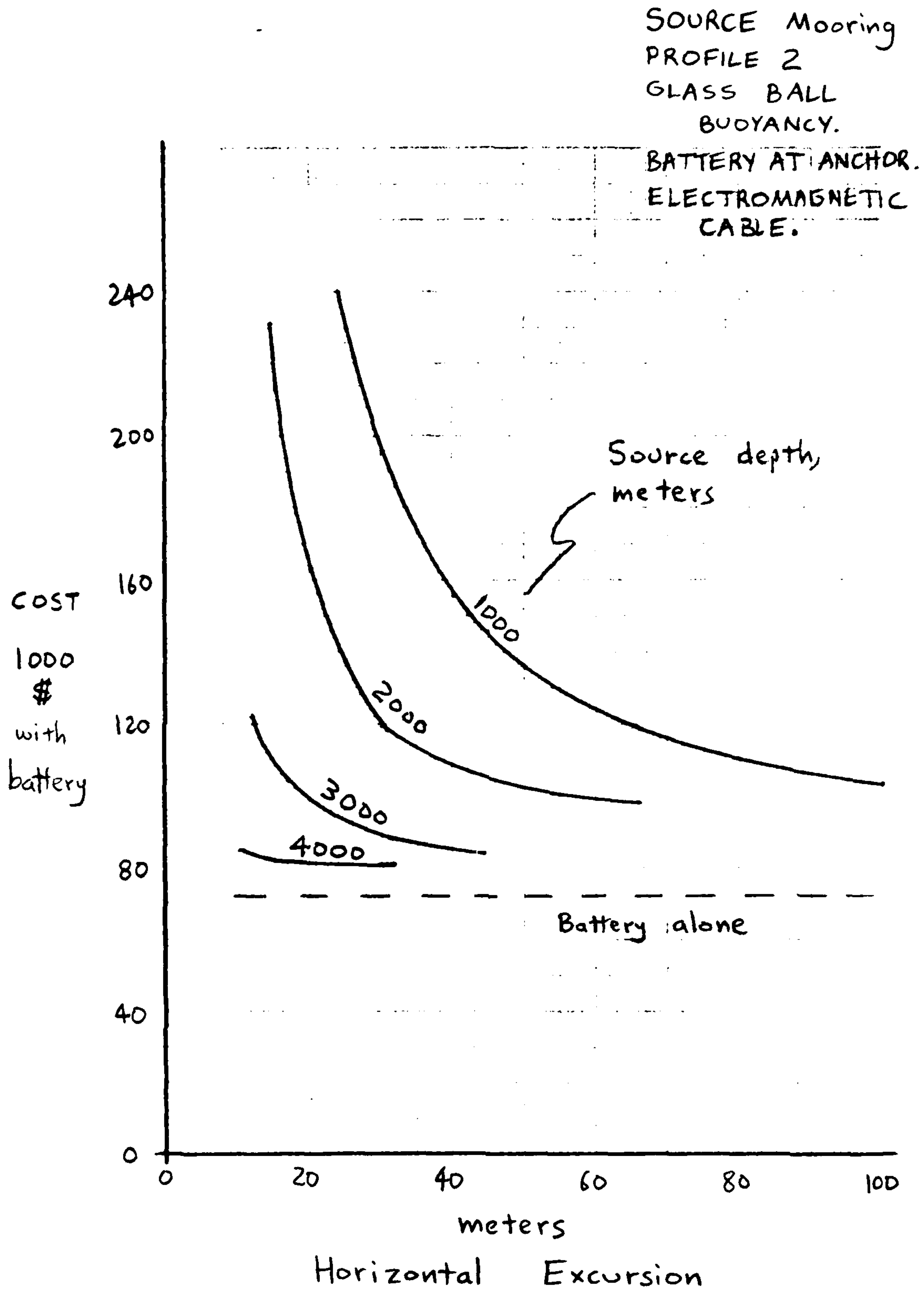

FIGURE 19

Cost vs. excursion, depth for mooring design AS8 under current profile 2.

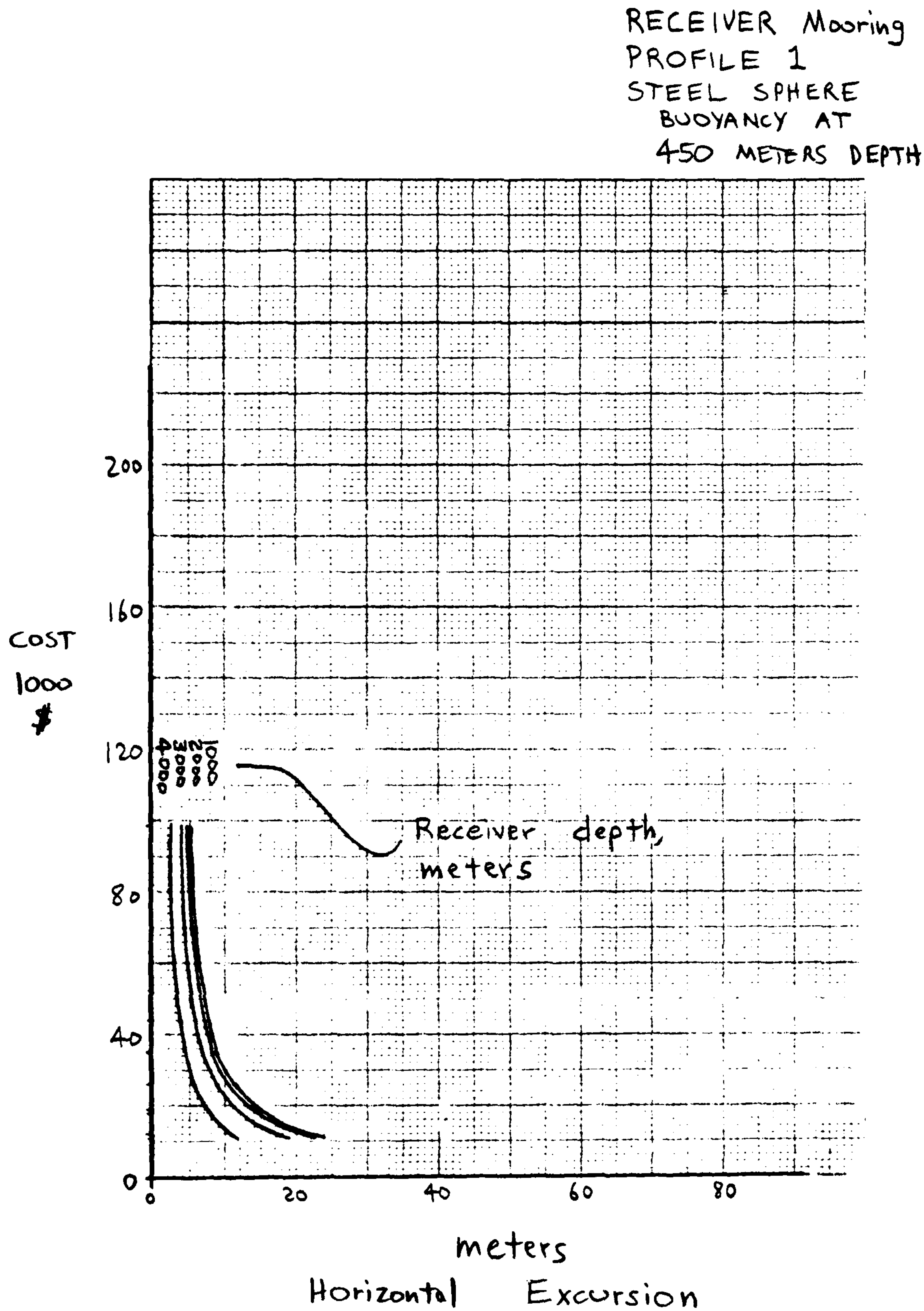

FIGURE 20
Cost vs. excursion, depth for mooring design AR2 under current profile 1.

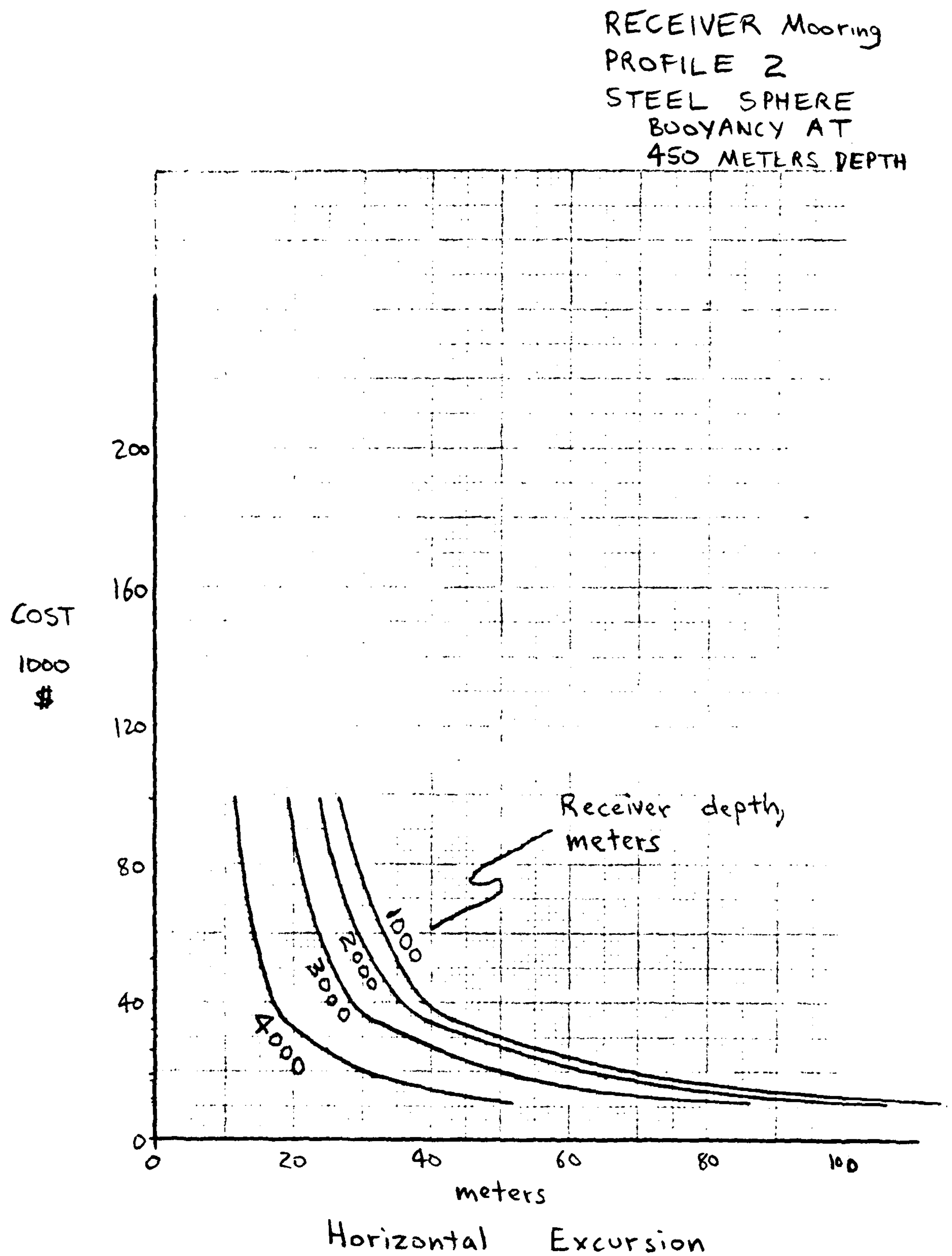

FIGURE 21

Cost vs. excursion, depth for mooring design AR2 under current profile 2.

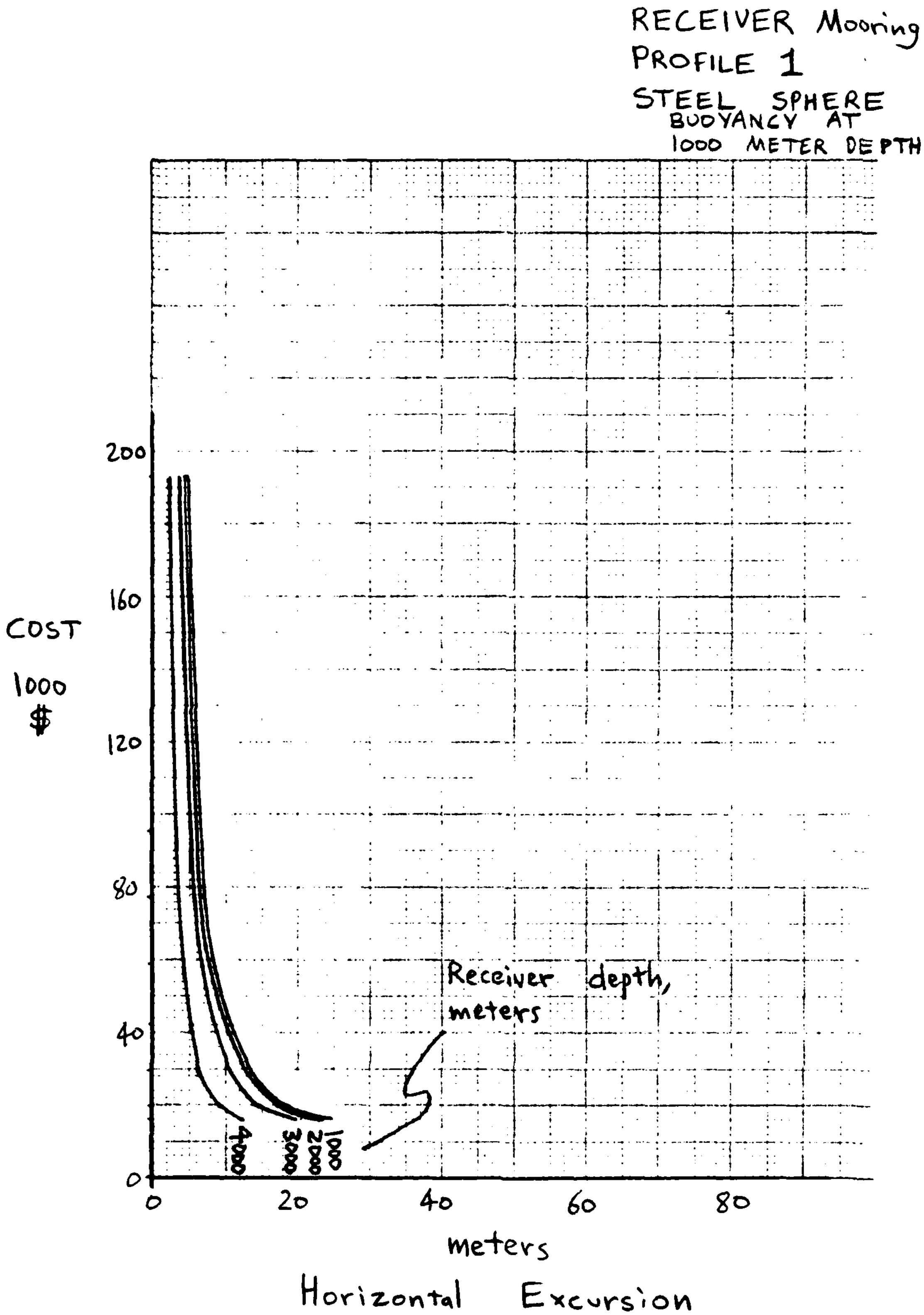

FIGURE 22

Cost vs. excursion, depth for mooring designs AR2 and AR3 under current profile 1.

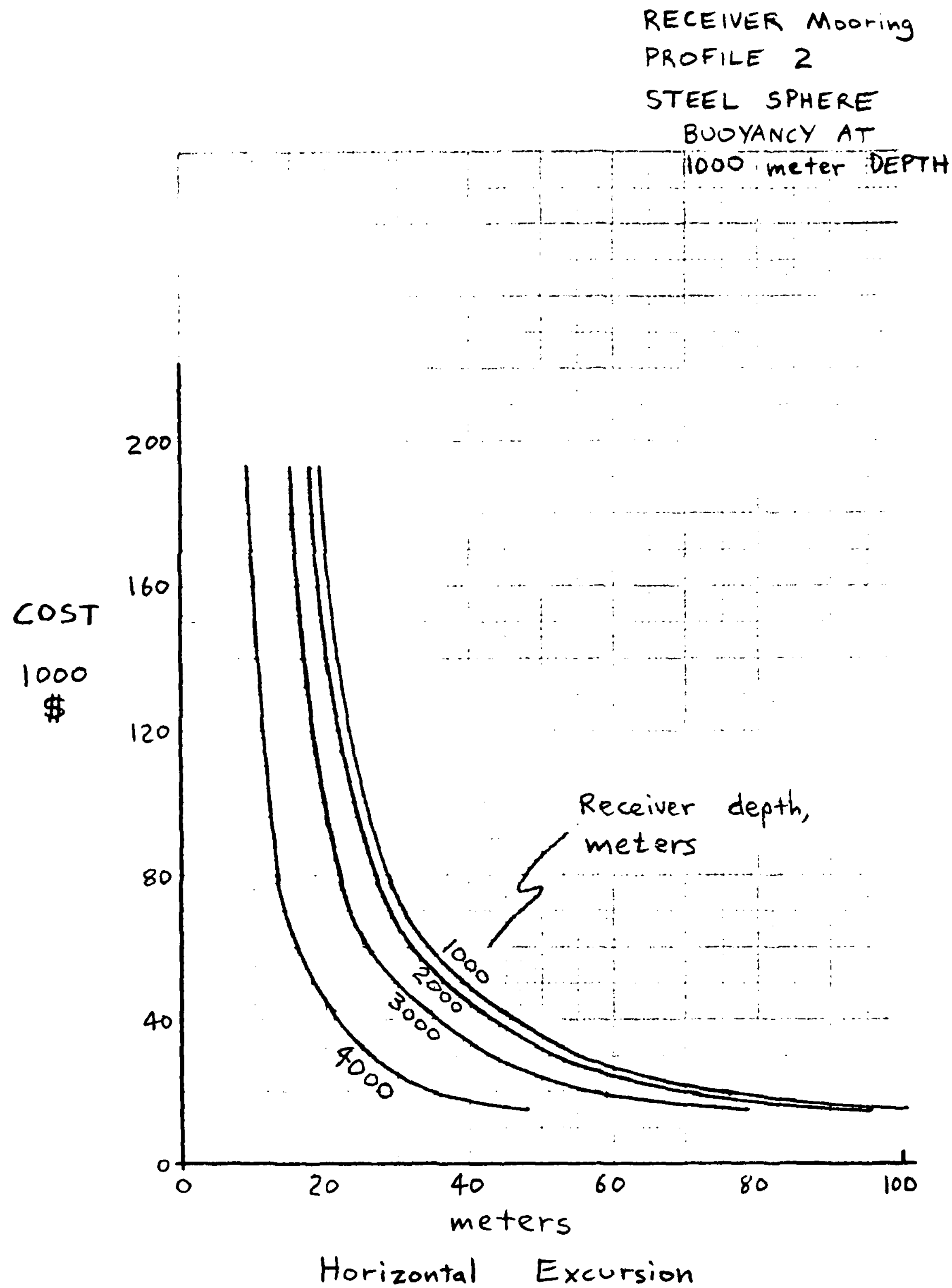

FIGURE 23

Cost vs. excursion, depth for mooring designs AR2 and AR3 under current profile 2.

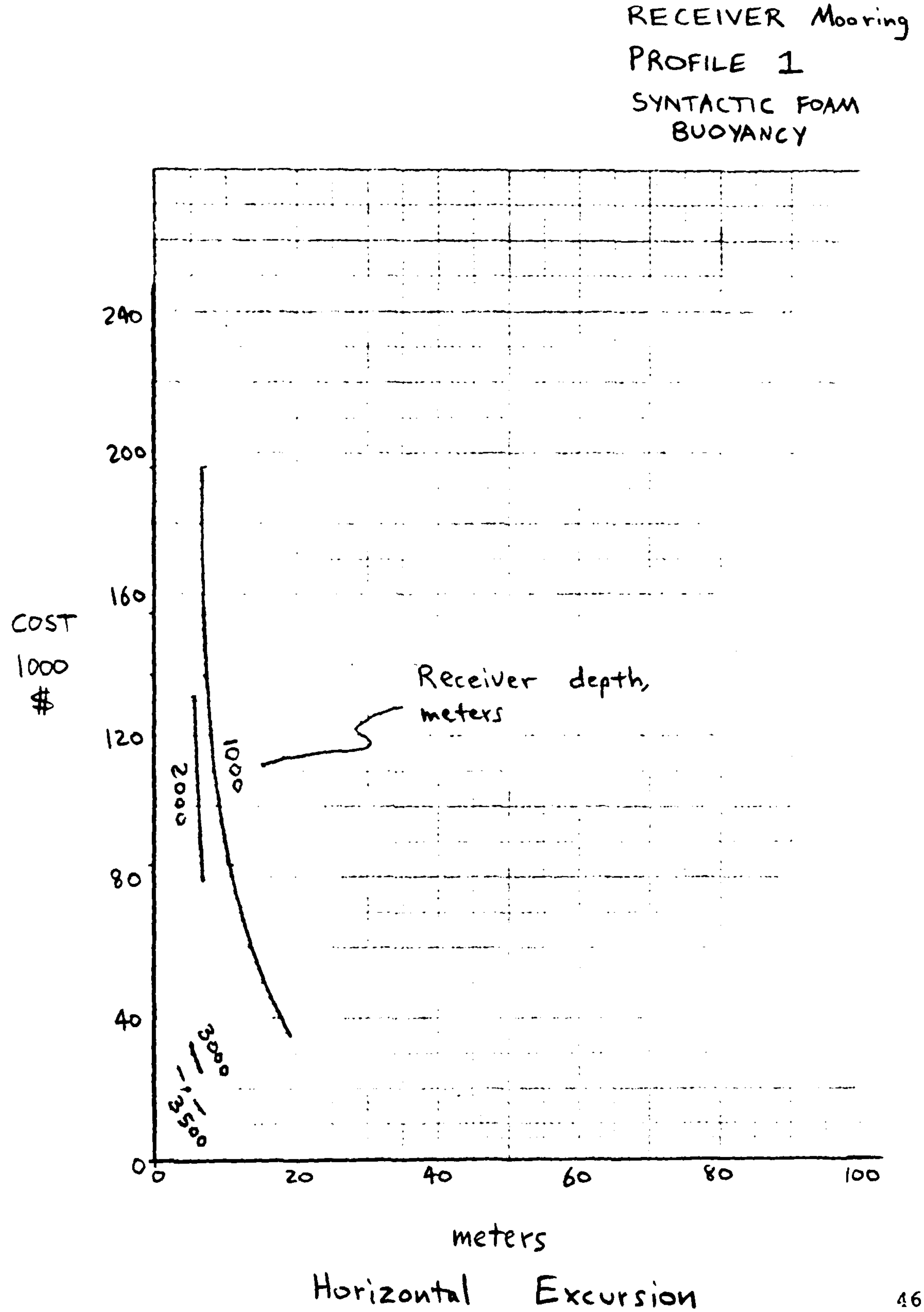

FIGURE 24
Cost vs. excursion, depth for mooring design AR1 under current profile 1.

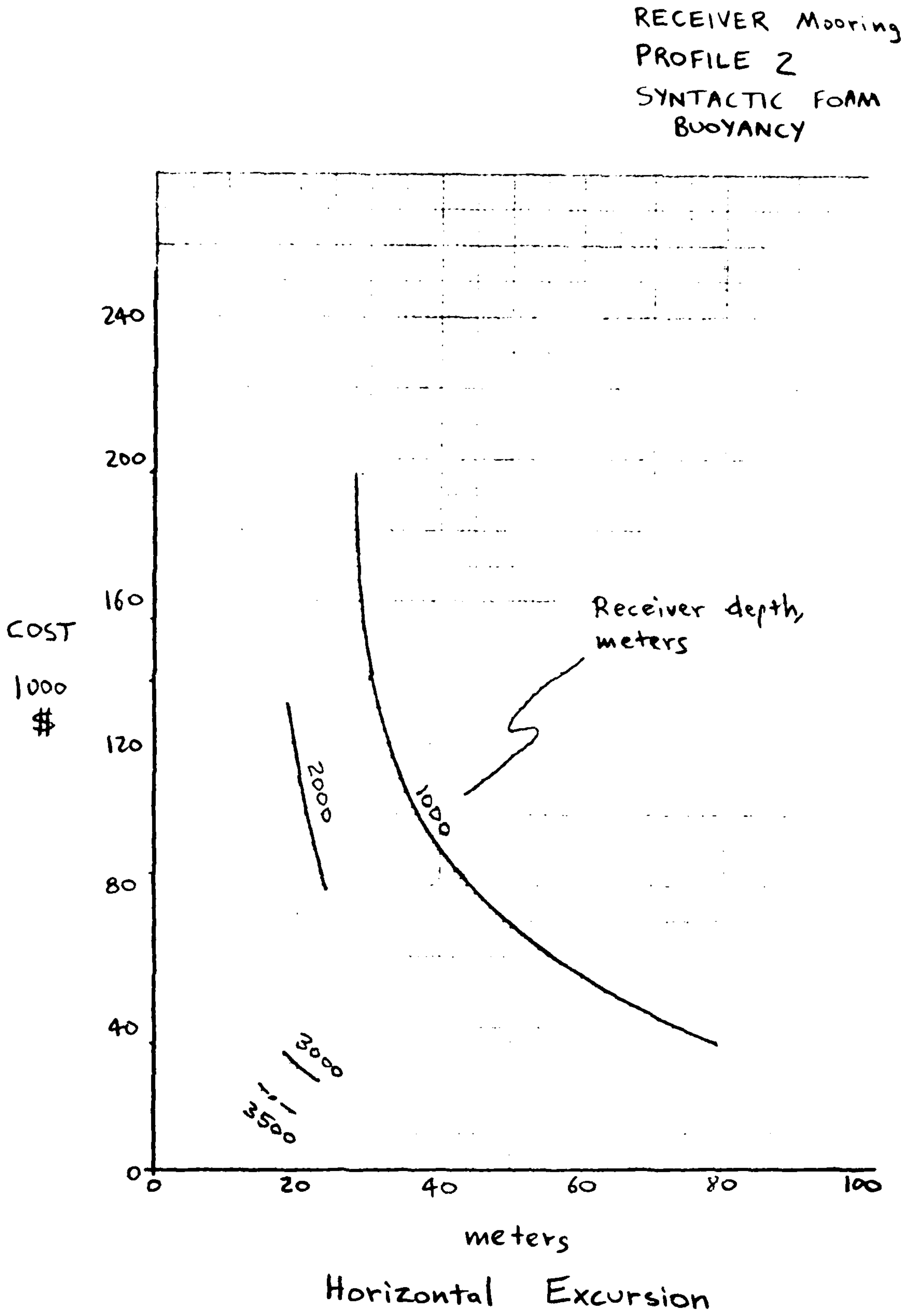

FIGURE 25
Cost vs. excursion, depth for mooring design AR1 under current profile 2.

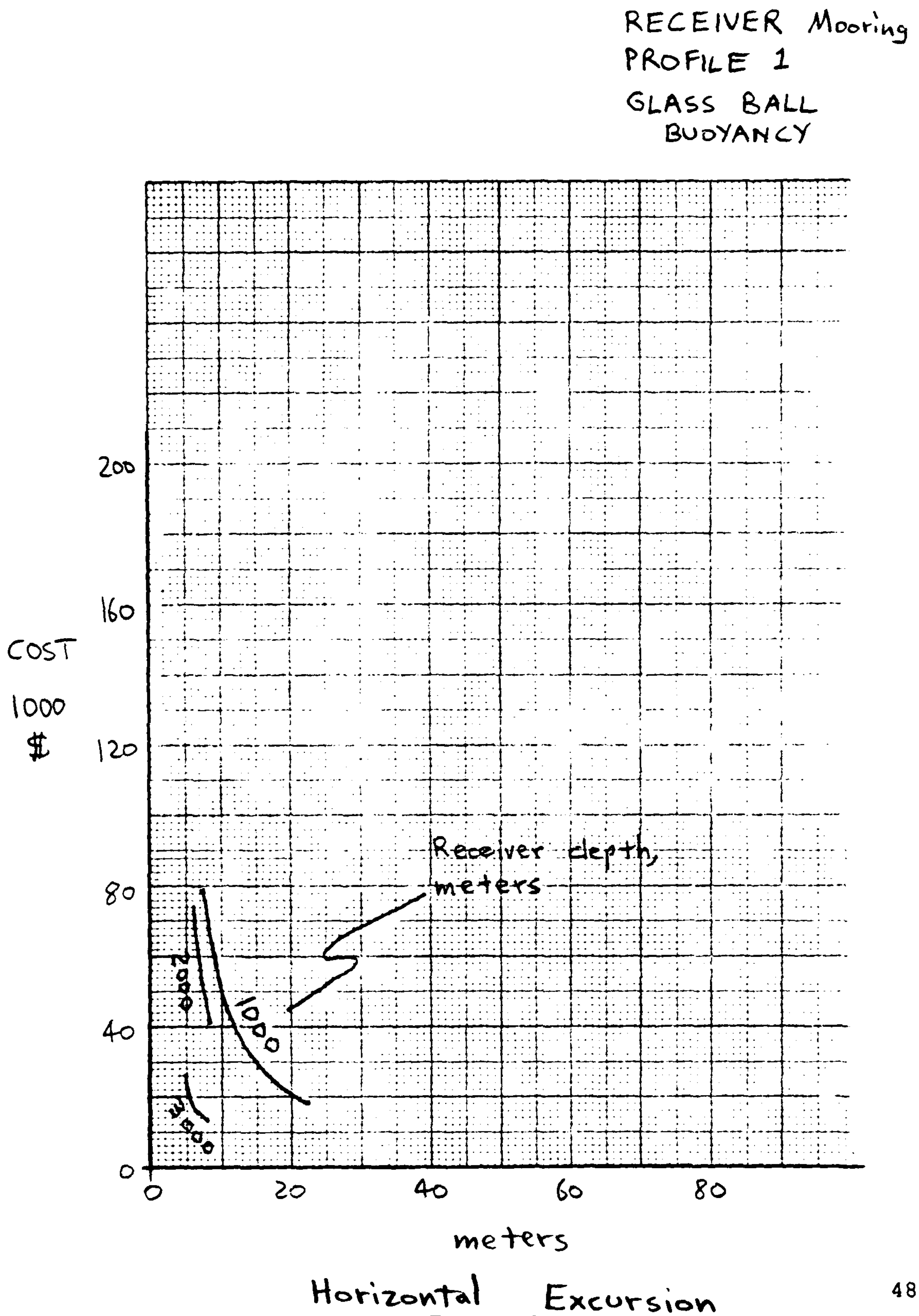

FIGURE 26
Cost vs. excursion, depth for mooring design AR4 under current profile 1.

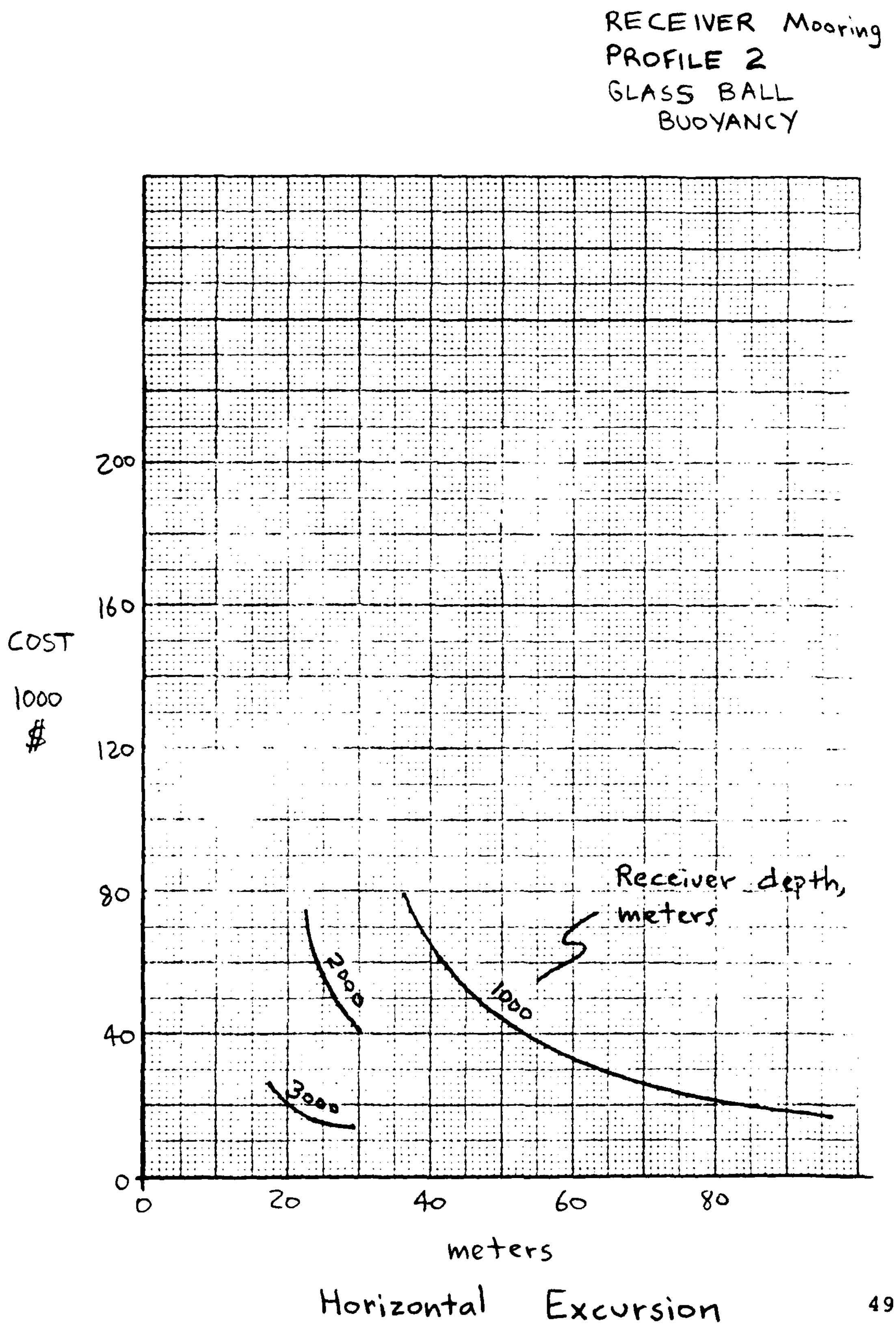

FIGURE 27
Cost vs. excursion, depth for mooring design AR4 under current profile 2.

APPENDIX A

Computer Simulation of Ocean Internal Wave Currents

A Fortran language computer program has been written to create synthetic time histories of North and East (u and v) components of ocean current. This is accomplished by applying an inverse Fast Fourier Transform (FFT) to spectra defined as follows:

> For frequencies greater than the Earth's inertial frequency, the amplitude is given by Equation 6-20 of Garrett and Munk (1972). For frequencies less than or equal to the intertial frequency, the amplitude is chosen to be proportional to frequency, providing a decline with a slope of two on a log-log scaled power spectral density plot. This choice is motivated by Figure 4 of Garrett and Munk reproduced here as Figure 1.
>
> Over the entire frequency range, spectral phase is chosen randomly, independently for each of the particular frequencies in the discrete spectrum that the FFT requires as input.
>
> The spectra for North and East components are each calculated separately in this fashion. They differ in phase, but not in amplitude.

After the spectrum generation and inverse FFT's are computed, a single sinusoid corresponding to the tidal current is added to the North and East velocity time histories. The tidal amplitude (uniform over depth) is assumed to be 5 cm/sec. (10 cm/sec. peak-to-peak) at zero phase angle, identically for both the u and v components. Its period is 12.45 hours.

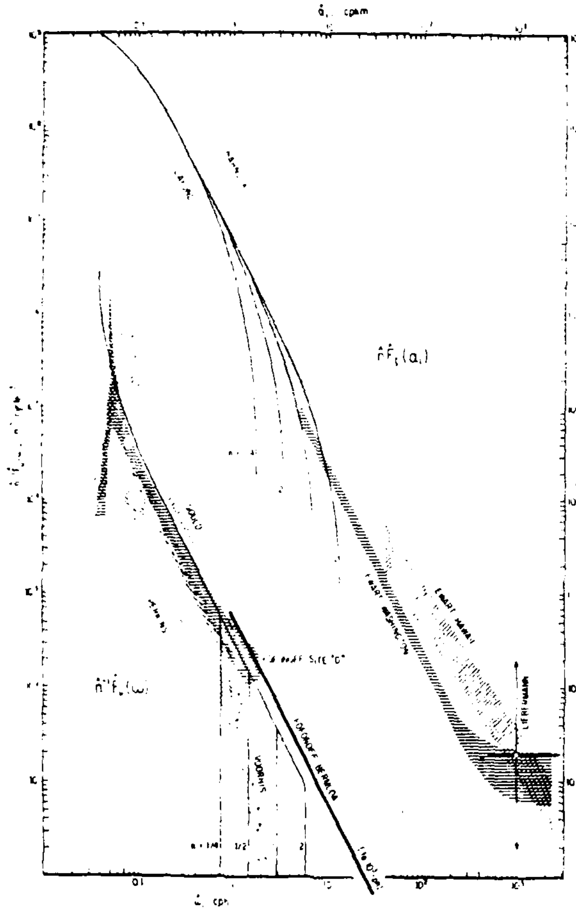

FIGURE 4 Bands represent the observed moored and floating spectra (Left, see Table 1) and towed spectra (Right, see Table 2). Dotted bands are presumably not subject to fine-structure noise. Curves are the derived relations (6.20, 21).

(Taken from Garrett and Munk 1972)

Figure 1

Equations

1. Spectrum if $\omega > \omega_I$:

Equation 6-20 of Garrett and Munk can be rewritten as:

$$F^2(\omega) = 8062.35\omega_{VB}\omega_I \frac{1 + \frac{\omega_I^2}{\omega^2}}{\sqrt{1 - \frac{\omega_I^2}{\omega^2}}} \cdot \frac{1}{\omega^2}$$

where $F^2(\omega)$ is the amplitude squared, (meter^2/hour^2/CPH)

ω is frequency (CPH),

ω_I is the Earth's inertial frequency (CPH),

ω_{VB} is the Vaisala-Brunt frequency (CPH).

Intuitively, this equation can be divided into three parts:

1. A semi-empirical scale factor, $8062.35\omega_{VB}\omega_I$.

2. An ideal degenerate functional dependence, $\frac{1}{\omega^2}$.

   This produces the familiar -2 spectral slope on a log-log PSD plot.

3. A slope-modifying term,

$$\frac{1 + \frac{\omega_I^2}{\omega^2}}{\sqrt{1 - \frac{\omega_I^2}{\omega^2}}}$$

This approximates unity when $\omega >> \omega_I$, and serves to produce an upsweep in amplitude as ω nears ω_I. This upsweep is not tame; the amplitude is infinite at $\omega = \omega_I$. This is no problem so long as one considers the continuous spectra, because the area under the peak is finite. However, the peak could cause a large phantom excess of power to appear in a discretely sampled spectrum; If a sampled value of ω happens to be very close to ω_I, the computed power contribution $F^2(\omega)\Delta\omega$ will be huge! As insurance against this hazard, the computer program places a ceiling of of 2000000 ω_{VB} on the value of $F^2(\omega)$.

2. Spectrum if $\omega \leq \omega_I$:

$$F^2(\omega) = 2000000 \frac{\omega^2}{\omega_I^2}$$

3. Earth's Inertial Frequency:

$$\omega_I = \frac{\sin\text{ (latitude)}}{12}$$

4. Vaisala-Brunt Frequency:

$\omega_{VB} = 3$ cycles/hour, if Z > mixing layer depth

$\omega_{VB} = 3\ e^{\frac{-Z}{1300}}$ if $Z \leq$ mixing layer depth

where Z is the depth in meters.

Computer Program Notes

The present program is an extensively revised and corrected version of one written by Marvin Gove of NORDA. (The most important change consisted of applying the FFT scale factor $\Delta\omega = \frac{1}{\text{total time of data}}$ to power rather than amplitude.)

The program accepts the following parameters as input:

Title.
Number of depths (separate time histories to be made for each).
Depths (number as above).
Latitude.
Time increment desired for u, v histories.
Total time desired for u, v histories.
Mixed layer depth.

The program has been verified by "closing the loop", using a previously written Power Spectral Density (PSD) program to re-create the original spectrum from the generated u and v time series. At each stage of the process the total power has been calculated and observed not to change. Figures 2 and 3 are sample log-log PSD plots of North velocity histories generated by the program. They conform well with Figure 1, the ideal spectrum from Garrett and Munk. Note that in all three plots, the power axis has been scaled by the Vaisala-Brunt frequency, so as to make the curves depth-independent. They are still latitude-dependent, however.

Figure 4 is a program listing. Figure 5 is a sample program output.

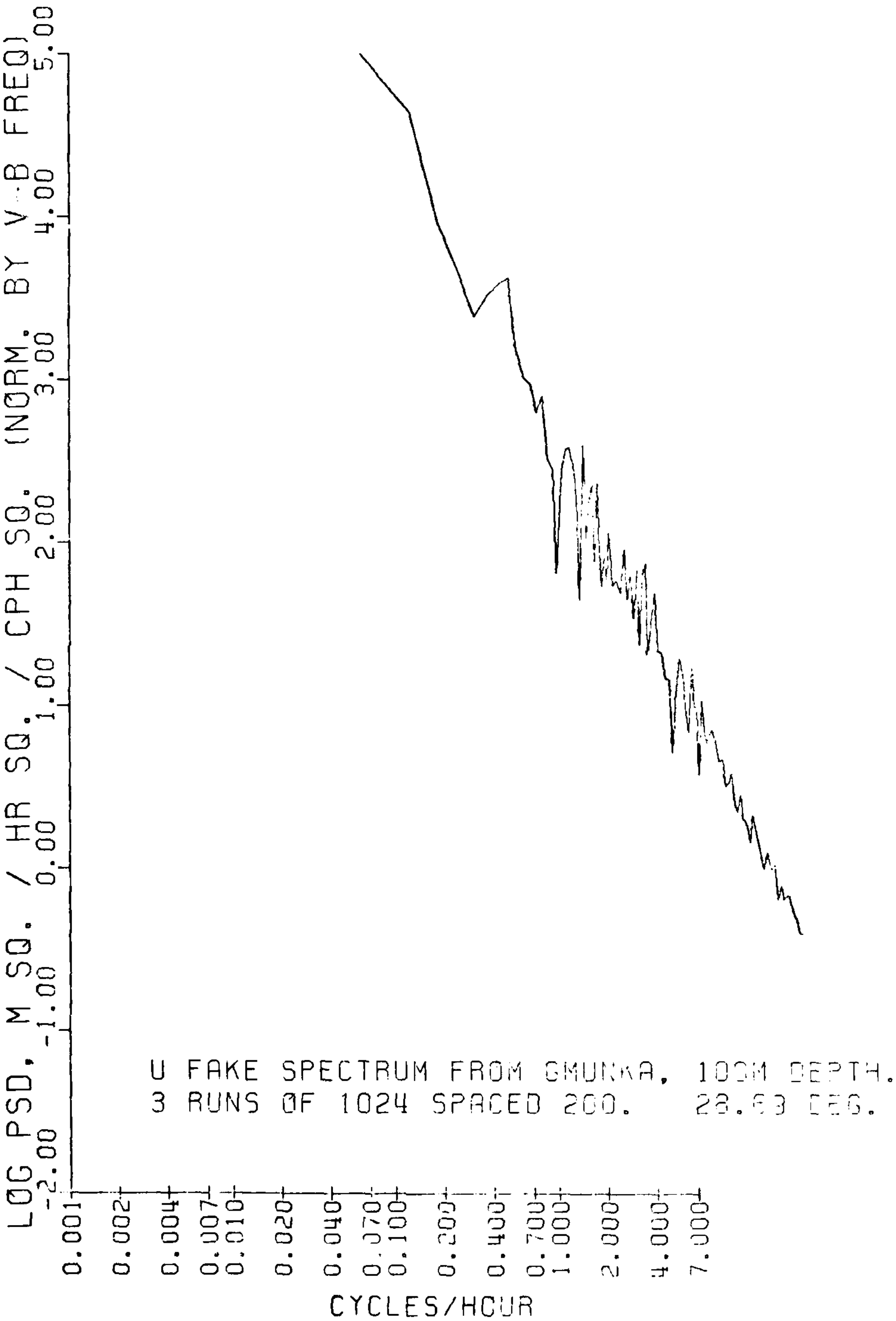
LOG PSD, M SQ. / HR SQ. / CPH SQ. (NORM. BY V-B FREQ)
U FAKE SPECTRUM FROM
3 RUNS OF 1024 SPACED 200.
CYCLES/HOUR

Figure 2

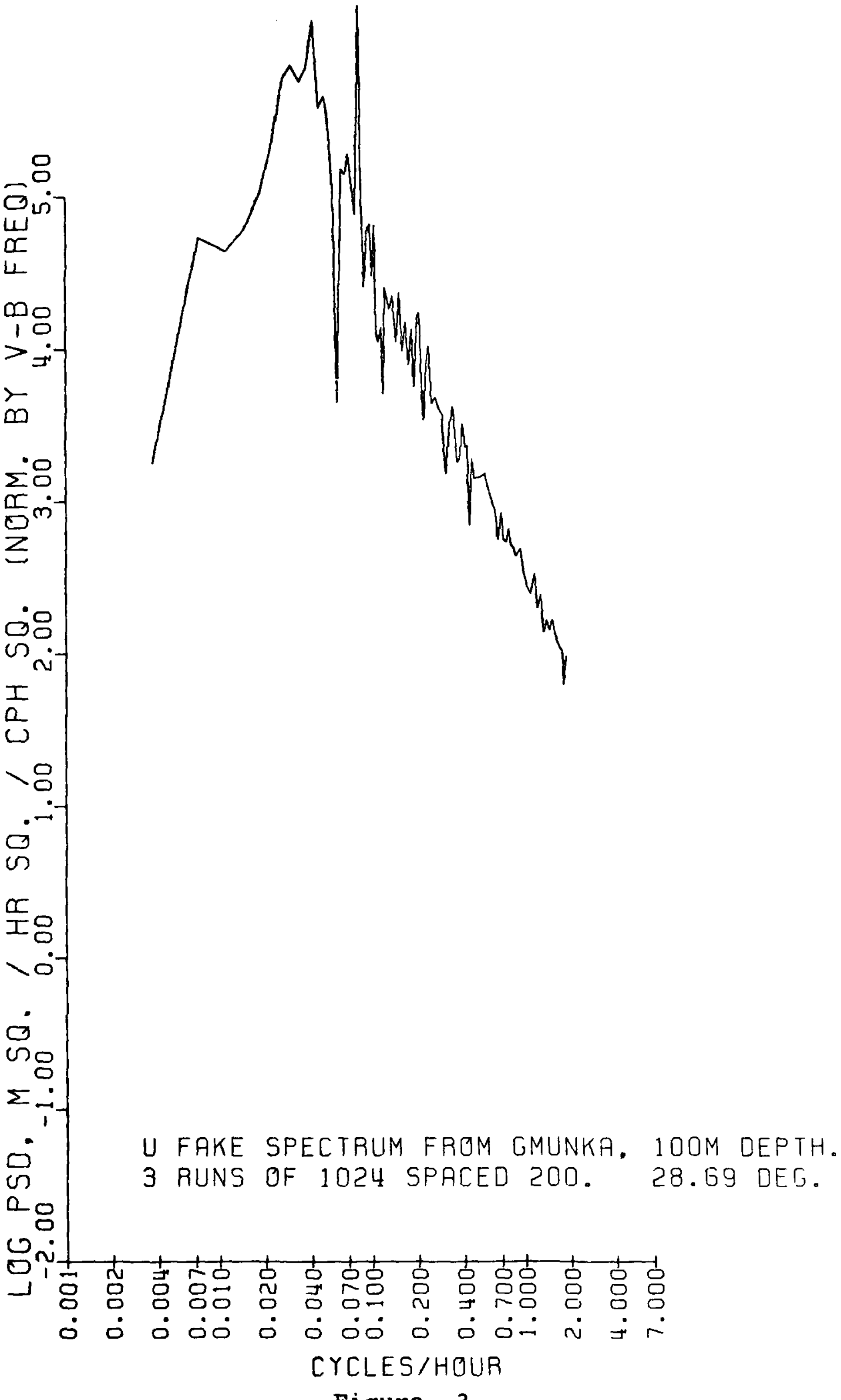

LOG PSD, M SQ. / HR SQ. / CPH SQ. (NORM. BY V-B FREQ)
-2.00
-1.00
0.00
1.00
2.00
3.00
4.00
5.00
U FAKE SPECTRUM FROM GMUNKA, 100M DEPTH.
3 RUNS OF 1024 SPACED 200. 28.69 DEG.
0.001
0.002
0.004
0.007
0.010
0.020
0.040
0.070
0.100
0.200
0.400
0.700
1.000
2.000
4.000
7.000
CYCLES/HOUR

Figure 3

```
      C
      C     THIS PROGRAM COMPUTES UNCORRELATED HORIZONTAL VELOCITY COMPONENTS
      C     DUE TO INTERNAL WAVE MOTION BY EVALUATING THE INVERSE FAST
      C     FOURIER TRANSFORM OF THE GARRETT-MUNK SPECTRUM AT A GIVEN DEPTH.
      C     AN EXPONENTIAL DECAY BELOW THE MIXED LAYER IS ASSUMED FOR THE
      C     VAISALA-BRUNT FREQUENCY.
      C
      C     INPUTS ARE:
      C         LABLE(L) = HEADER IN 12A4 FORMAT.
      C              JMAX = NUMBER OF DEPTHS (10 MAXIMUM).
      C              XLAT = LATITUDE (DEGREES).
      C              TMAX = MAXIMUM TIME (SECONDS).
      C              DELT = TIME INCREMENT (SECONDS) FOR FFT.
      C             ZMIXL = MIXED LAYER DEPTH (METERS).
      C              Z(J) = DEPTHS (METERS).
      C
      C     OUTPUT FOR EACH DEPTH IS KMAX SETS OF:
      C         TIME (HOURS),
      C         HORIZONTAL VELOCITY COMPONENTS U AND V (METERS/SECOND).
      C         (WHERE KMAX IS THE LARGEST POWER OF 2 THAT IS <= TMAX/DELT.)
      C
      C     THIS PROGRAM WAS WRITTEN BY JIM SCHOLTEN OF CSDL DURING MAY-JULY
      C     1980.   IT IS AN EXTENSIVELY REVISED VERSION OF A PROGRAM BY
      C     MARVIN GOVE OF NORDA.
      C
      C
      C
ISN 0002    REAL*8  RNDMR, WIDTH
ISN 0003    REAL*4  FU2(4097), U(8192), V(8192), F(2,4096),
           1        LABLE(12), Z(10), VBFH(10),
           2        L1(10), L2(10,5), L3(10,5), MTENT, NTENT
ISN 0004    INTEGER*4  KMAX, NN(1)
ISN 0005    EQUIVALENCE (KMAX, NN(1))
ISN 0006    DATA  PI,  DTOR/
           1     3.145926,   .0174533 /
ISN 0007    WIDTH = 1.D00
ISN 0008    PTOT1 = 0.
ISN 0009    PTOT2 = 0.
      C
      C**********   COMPUTE GARRETT-MUNK COEFFICIENT  (EQUATION 6-20)   ******
      C
ISN 0010      E = 2. * PI * 1.E-5
      C  E IS DIMENSIONLESS.
ISN 0011      NTENT = 3.
      C  NTENT IS CYCLES PER HOUR, GARRETT-MUNK NORMALIZATION FACTOR FOR FREQ.
ISN 0012      MTENT = 0.122E-3
      C  MTENT IS CYCLES PER METER
ISN 0013      COEFF = 2. * E * NTENT / (PI * MTENT ** 2)
      C
      C
      C
      C**********    INPUTS   **********
      C
```

Figure 4

```
ISN 0014          READ (5,5) (LABLE(L),L=1,12)
ISN 0015        5 FORMAT (12A4)
ISN 0016          READ (5,*) JMAX, XLAT, DELT, TMAX, ZMIXL
ISN 0017          READ (5,*) (Z(J),J=1,JMAX)
            C
            C****************************************************************
            C
ISN 0018          WRITE (6,6) (LABLE(L),L=1,12)
ISN 0019        6 FORMAT (1H1, 10X, 12A4)
ISN 0020          WRITE (6,15) JMAX, XLAT, DELT, TMAX, ZMIXL
ISN 0021       15 FORMAT (5X, 'NO. DEPTHS =', ,I3, 5X, 'LAT (DEG) =', F10.3,
                1        5X, 'DELT (S) =', F10.1, 5X, 'TMAX (S) =', F10.1,
                2        5X, 'ZMIXL (M) =', F10.3, 5X,/)
ISN 0022          WRITE (6,32)  COEFF
ISN 0023       32 FORMAT ('     GARRETT-MUNK COEFFICIENT (M SQ./HR./CYCLE) =',F12.2)
            C
            C**********   COMPUTE INERTIAL FREQUENCY.
            C
ISN 0024          CMI =  SIN( XLAT*DTOR ) / 12.
            C          CMI IS CYCLES/HOUR.
ISN 0025          WRITE (6,31)  CMI
ISN 0026       31 FORMAT (/'     INERTIAL FREQUENCY IS (CPH):',F10.6)
ISN 0027          TWOPI = PI * 2.
ISN 0028          CMI2 = CMI * CMI
            C
ISN 0029          KMAX = INT( TMAX / DELT )
ISN 0030          DO 24 I = 8,14
ISN 0031          J = 2**I
ISN 0032          IF (J .GT. KMAX) GO TO 27
ISN 0034       24 CONTINUE
ISN 0035       27 KMAX = J/2
ISN 0036          SQKM = SQRT(FLOAT(KMAX))
ISN 0037          KF = KMAX / 2 + 1
ISN 0038          TT = DELT * KMAX / 3600.
            C   TT IS IN HOURS.
ISN 0039          DELCM = 1 / TT
            C          DELCM IS CYCLES PER HOUR.
            C
            C**********   BEGIN DEPTH LOOP   **********
            C
ISN 0040          DO 200 J = 1,JMAX
            C
            C**********   COMPUTE LOCAL VAISALA-BRUNT FREQUENCY   ***********
            C
ISN 0041          IF (Z(J) .GT. ZMIXL)  GO TO 25
ISN 0043          VBFH(J) = 3.
ISN 0044          GO TO 26
ISN 0045       25 VBFH(J) = 3. * EXP(-Z(J)/1300.)
            C          VBFH IS CYCLES/HOUR.
ISN 0046       26 CONTINUE
ISN 0047          WRITE (6,30) Z(J), VBFH(J), KMAX
ISN 0048       30 FORMAT (1H0, 19X, 'DEPTH (M) =', F10.3, 5X, 'VB FREQ (CPH) =',
                1          F10.3, '      KMAX =', I10,
                2          //20X, 'TIME(HRS)', 8X, 'U(MPS)',11X, 'V(MPS)'/)
            C
ISN 0049          FU2(1) = 0.
ISN 0050          OM = 0.
            C
```

Figure 4 cont'd.

```
                C*******    LOAD FU2(K) WITH GARRET-MUNK SPECTRUM MODIFIED
                C           TO PROVIDE FINITE VALUES FOR FREQUENCIES LESS THAN
                C           THE INERTIAL FREQUENCY.
                C
ISN 0051              DO 100 K = 2,KF
ISN 0052              CM = CM + DELCM
ISN 0053              CM2 = CM * CM
ISN 0054              IF (CM .GT. CMI)  GO TO 90
ISN 0055              FU2(K) = 2000000. * CM2 / CMI2
                C          FU2(K) IS METERS SQUARED / HOUR SQUARED / CPH.
ISN 0057              GO TO 95
ISN 0058           90 CMRAT = CMI2 / CM2
ISN 0059              FU2(K) = COEFF * CMI * (1.+CMRAT) / (SQRT(1.-CMRAT)*CM2)
ISN 0060              IF (FU2(K) .GT. 2.E6)    FU2(K) = 2.E6
ISN 0062              FU2(K) = FU2(K) * VEFH(J)
ISN 0063           95 CONTINUE
                C   WRITE CPH AND AMPLITUDE**2 FOR DEBUGGING.
                C     WRITE (6,51) CM, FU2(K)
                C  51 FORMAT (2F15.6)
ISN 0064          100 CONTINUE
                C
                C*******    LOAD U AND V WITH RANDOM NUMBERS BETWEEN 0 AND 1, TO
                C           BE USED IN ASSIGNING PHASES.
                C
ISN 0065              DO 50 K = 1,KF
ISN 0066              U(K) = 0.5E0 + RNDMR(WIDTH)
ISN 0067              V(K) = 0.5E0 + RNDMR(WIDTH)
ISN 0068          50  CONTINUE
                C
                C*******    ASSIGN RANDOM PHASE FACTOR AND GIVE REQUIRED
                C           SYMMETRY TO REAL AND IMAGINARY COMPONENTS OF
                C           U SPECTRUM.
                C
ISN 0069              DO 120 K = 1,KMAX
ISN 0070              IF (K .GT. KF) GO TO 115
ISN 0072              PHASE = TWOPI * U(K)
                C    THE 2 FACTOR BELOW IS TO COMPENSATE FOR SPLITTING THE AMPLITUDE
                C       AT EACH FREQUENCY INTO TWO PIECES OF 1/2 AMPLITUDE,
                C       AS REQUIRED BY THE FFT.
ISN 0073              FU = SQRT (  FU2(K) / 2. / TT  )
ISN 0074              F(1,K) = COS(PHASE) * FU
ISN 0075              F(2,K) = SIN(PHASE) * FU
ISN 0076              GO TO 121
ISN 0077          115 KI = 2 * KF - K
ISN 0078              F(1,K) = F(1,KI)
ISN 0079              F(2,K) = -F(2,KI)
                C    THE 2 FACTOR BELOW IS TO COMPENSATE FOR SPLITTING THE AMPLITUDE
                C       AT EACH FREQUENCY INTO TWO PIECES OF 1/2 AMPLITUDE,
                C       AS REQUIRED BY THE FFT.
ISN 0080          121 PTOT1 = PTOT1 + 0.5 * (F(1,K)**2 + F(2,K)**2) * 2.0
ISN 0081          120 CONTINUE
                C
                C     WRITE (6,167) ((F(I,JJ),I=1,2),JJ=1,2048,8)
                C     WRITE (6,167)
ISN 0082          167 FORMAT (8E15.6)
                C
                C
                C*******    BRING IN INVERSE FFT TO COMPUTE U FROM ITS SPECTRUM.
```

Figure 4 cont'd.

```
                C
ISN 0083              CALL FOURT (F, NN, 1, +1, 1, 0)
                C
                C     WRITE (6,167) ((F(I,JJ),I=1,2),JJ=1,2048,8)
                C     WRITE (6,167)
                C
ISN 0084              DO 140 K = 1,KMAX
ISN 0085              U(K) = F(1,K)
ISN 0086              PTOT2 = PTOT2 + U(K)**2
ISN 0087          140 CONTINUE
ISN 0088              PTOT2 = PTOT2 / KMAX
                C
                C   DO FFT AGAIN FOR TEST.
                C     CALL FOURT (F,NN,1,-1,1,0)
                C     WRITE (6,167) ((F(I,JJ),I=1,2),JJ=1,2048,8)
                C     WRITE (6,167)
                C
                C*******   REPEAT FOR V COMPONENT.
                C
ISN 0089              DO 145 K = 1,KMAX
ISN 0090              IF (K .GT. KF) GO TO 135
ISN 0092              PHASE = TWOPI * V(K)
ISN 0093              FU = SQRT( FU2(K) / 2. / TT)
ISN 0094              F(1,K) = COS(PHASE) * FU
ISN 0095              F(2,K) = SIN(PHASE) * FU
ISN 0096              GO TO 145
ISN 0097          135 KI = 2 * KF - K
ISN 0098              F(1,K) = F(1,KI)
ISN 0099              F(2,K) = -F(2,KI)
ISN 0100          145 CONTINUE
                C
ISN 0101              CALL FOURT (F, NN, 1, +1, 1, 0)
                C
                C******    ADD M2 BAROTROPIC TIDAL COMPONENT.
                C
ISN 0102              DO 150 K = 1,KMAX
ISN 0103              V(K) = F(1,K)
ISN 0104              TM2 = 0.05 * SIN(1.405257E-4 * DELT * (K-1))
                C           TM2 IS METERS/SECOND.        PERIOD IS 12.45 HOURS.
                C   CONVERT U AND V TO M/SEC FROM M/HOUR:
ISN 0105              U(K) =  U(K) / 3600. +  TM2
ISN 0106              V(K) =  V(K) / 3600. +  TM2
ISN 0107          150 CONTINUE
                C
                C**********   OUTPUT   **********
                C
ISN 0108              DO 200 K = 1,KMAX
ISN 0109              T = FLOAT(K) * DELT / 3600.
                C           T IS HOURS.
ISN 0110              WRITE (10) (T, U(K), V(K))
ISN 0111              IF (K .GT. 45)  GO TO 200
ISN 0113          160 WRITE (6,165) T, U(K), V(K)
ISN 0114          165 FORMAT  (20X, 3(F12.5, 5X))
ISN 0115          200 CONTINUE
ISN 0116              WRITE (6,166)  (PTOT1, PTOT2)
ISN 0117          166 FORMAT (//' U POWERS BEFORE AND AFTER INVERSE FFT ARE :',
                     1        2E15.6, '  M**2 / H**2.',//)
ISN 0118              STOP
```

Figure 4 cont'd.

TEST RUN NUMBER A10, 2048 POINTS

NO. DEPTHS = 1 LAT (DEG) = 28.690 DELT (S) = 960.0 TMAX (S) = 1966080.0

GARRETT-MUNK COEFFICIENT (M SQ./HR./CYCLE) = 8062.35 ZMIXL (M) = 50.000

INERTIAL FREQUENCY IS (CPH): 0.040006

DEPTH (M) = 100.000 VB FREQ (CPH) = 2.773 NMAX = 20.0

TIME(HRS)	U(MPS)	V(MPS)
0.26667	-0.03049	-0.05726
0.53333	-0.02139	-0.03700
0.80000	[illegible]	-0.03229
1.06667	-0.07116	0.01458
1.33333	-0.02737	-0.00722
1.60000	-0.03311	0.00737
1.86667	-0.04191	0.00721
2.13333	-0.04324	0.01290
2.40000	-0.00335	0.03348
2.66667	-0.02000	0.06270
2.93333	-0.02340	0.07676
3.20000	0.00615	0.09275
3.46667	0.01611	0.09226
3.73333	0.07026	0.07331
4.00000	0.07153	0.07370
4.26667	0.08309	0.07079
4.53333	0.07619	0.07560
4.80000	0.05914	0.05394
5.06667	0.02886	0.04579
5.33333	-0.00036	0.03725
5.60000	-0.01018	0.02540
5.86667	-0.04975	0.00166
6.13333	-0.03662	-0.03131
6.40000	-0.04926	-0.03220
6.66667	-0.03724	-0.03223
6.93333	-0.03237	-0.04241
7.20000	-0.00070	-0.03463
7.46667	0.01123	-0.04027
7.73333	0.01673	-0.02571
8.00000	0.00092	-0.03326
8.26667	0.02215	-0.04273
8.53333	0.02623	-0.07295
8.80000	0.00174	-0.04022
9.06667	-0.00201	-0.01612
9.33333	-0.01917	-0.03393
9.60000	-0.02398	-0.05148
9.86667	-0.02115	-0.06580
10.13333	-0.01009	-0.06014
10.40000	0.01234	-0.03543
10.66667	0.02305	-0.03324
10.93333	0.04249	0.00519
11.20000	0.07170	-0.00230
11.46667	0.10077	0.00975
11.73333	0.10561	-0.00400
12.00000	0.10724	0.00440

U POWERS BEFORE AND AFTER INVERSE FFT ARE : 0.769181E+05 0.769186E+05 M**2 / H**2.

Figure 5

APPENDIX B

Power Systems for the Long-Range Acoustic Transmitter

STRAWMAN #1

Lithium Primary Battery
Lithium Thionyl Chloride ($LiSOCl_2$)

Assumptions

(a) Energy required is 85 KWH derived as follows:

(1) 2-year life, 200 watts peak electrical power required during acoustic transmission, 0.5 watts standby power at all times, 3 minute acoustic transmission every hour over a 24-hour period, then a 48-hour rest. All of these parameters may be eased based on future sea tests.

(2) A precision time reference (clock) is required. There is some evidence at hand that a suitable one might be obtained requiring 1 watt or less (continuously). Assume 1 watt.

Therefore: $\text{AVG PWR} = (\frac{1}{3})\ (\frac{3}{60})\ (200) + 1.5 = 4.84\ \text{WATT}$

$$\text{TOT ENERGY} = \frac{(4.84)\ (2)\ (365)\ (24)}{1000} = 85\ \text{KWH}$$

(b) Use ALTUS battery stack of 17-inch diameter cells (cells are available in various capacities and thicknesses between 0.5 and 7.35 inches). Average energy density is 180 WH/lb. and 15 WH/inch^3.

(c) Battery contained in a cylindrical pressure vessel formed from ASTM A285 Grade C pressure vessel quality

hot-rolled steel plate. Working stress is 27,000 psi. Assume the vessel has hemispherical end bells. Vessel walls will be so thick that buckling is not a problem (see analysis in Appendix D). Cylinder inside diameter is 18 inches.

(d) Pressure vessel cost is approximately 3 dollars per pound (based on current prices and quantity production).

(e) Battery cost per ALTUS estimate on 5 June 1980:

one unit :	$100,000
10 units:	70,000 ea
25 units:	40,000 ea

Calculations

Battery volume = 5700 cubic inches; length = 25 inches
Cylinder length is therefore 26 inches
Battery weight = 470 pounds

An approximate stress analysis gives:

$$R_c = \frac{r_c}{1 - \frac{P}{\sigma}} \quad , \quad R_s = \frac{r_s}{\sqrt{1 - \frac{P}{\sigma}}}$$

where:

$R_{c/s}$ ≡ outside radius
$r_{c/s}$ ≡ inside radius (9-inches)
σ ≡ working compressive stress (27,000 psi)
P ≡ seawater pressure

P (psi) ≅ 1.46 x depth in meters

Results

Item/Depth (m)	1,000	2,000	3,000	4,000	5,000
Pressure (psi)	1,460	2,920	4,380	5,840	7,300
R_c (in)	9.51	10.09	10.74	11.48	12.34
R_s (in)	9.25	9.53	9.83	10.17	10.54
Vessel Wgt (lbs)	290	640	1,050	1,540	2,150
Total Wgt (lbs)	760	1,110	1,520	2,010	2,620
Seawater Displ (lbs)	400	440	500	560	640
Total Wgt in Water (lbs)	360	670	1,020	1,450	1,980
Vessel Cost* ($)	1,000	2,000	3,000	5,000	7,000
Total Cost* ($)	71,000	72,000	73,000	75,000	77,000
Added Cost of Floatation ($)	2,000	4,000	5,000	7,000	0 (useful anchor)

* assumes 10 - 25 units

Note

Published data by Mr. McCartney of NOSC, San Diego indicate that ALTUS batteries have performed well in ambient pressures up to 2000 psi. There is some hope, therefore, that a much lighter containment vessel might be used at depths in the 1000 - 2000 meter range.

STRAWMAN #2

Alkaline Primary Battery

Assumptions

(a) Energy required 85 KWH, as for Strawman #1

(b) Use E95 "D" size alkaline cells, V_{START} @ 1.5V, V_{END} @ .9V providing 9.28 AH (from pg. 310 of Ever-ready Handbook) @ 70°F. Derate 50% for 32°F service, thus assuming 4.64 AH @ 1.2V avg = 5.57 WH/cell. Each cell is 4.5 oz and 3.3 in^3. Therefore cell energy density = 19.8 WH/lb and 1.69 WH/in^3.

(c) Pressure vessel similar to that used for Strawman #1.

(d) "D" cell cost: $.65 ea. Add $.50 ea. for battery assembly.

Calculations

Total battery requires 15,300 cells weighing a total of 4,290 lb. and requiring 50,400 in^3 (excluding wiring, packaging and containment vessel). This assembly seems totally impractical, but we shall press on, nevertheless. Considering the large number of discrete cells to be packaged, assume a packaging efficiency of 75% and thus a total volume to be enclosed of 67,200 in^3 . Assume assembled pack weight = 4400 lbs.

Total battery cost is 15,300 x $1.15 = $17,600. There is no evidence that these cells can function at ambient seawater pressure, so the container must be a pressure vessel.

Using the same terminology defined for Strawman #1, we find the volume of steel in the pressure vessel is:

$$V_{cyl}\ \text{(cylinder volume)} = V_{bat} \left[\frac{1}{(1 - \frac{P}{\sigma})^2} - 1 \right]$$

$$V_{sph}\ \text{(end bells volume)} = \frac{4}{3} \pi r_s^3 \left[\frac{1}{(1 - \frac{P}{\sigma})^{3/2}} - 1 \right]$$

where V_{bat} is inside cylindrical volume for the battery (67,200 in^3).

Apparently the smaller r_s the smaller the weight. For example we find ($L \equiv$ cylinder length):

		1000 meters		5000 meters	
r_s(in)	L (in)	$V_{cyl}(in^3)$	$V_{sph}(in^3)$	$V_{cyl}(in^3)$	$V_{sph}(in^3)$
9	264	7,900	266	59,000	1,850
12	149	7,900	629	59,000	4,380
15	95	7,900	1,230	59,000	8,550
18	66	7,900	2,120	59,000	14,800

Since r_s has only a small influence on total weight, choose a convenient value for ease of manufacture and manageable length:

$$r_s = r_c = 18 \text{ inches}, \quad L = 66 \text{ inches}$$

We find:

Item/Depth (m)	1,000	2,000	3,000	4,000	5,000
Pressure (psi)	1,460	2,920	4,380	5,840	7,300
R_c (in)	19.03	20.18	21.49	22.97	24.67
R_s (in)	18.51	19.06	19.67	20.33	21.07
Vessel Wgt (lbs)	2,810	6,120	10,070	14,800	20,700
Total Wgt (lbs)	7,210	10,520	14,470	19,200	25,100
Seawater Displ (lbs)	3,760	4,200	4,720	5,350	6,120
Total Wgt. in Water (lbs)	3,450	6,320	9,750	13,850	18,980
Vessel Cost* ($)	8,000	18,000	30,000	44,000	62,000
Total Cost* ($)	26,000	36,000	48,000	62,000	80,000
Added Cost of Floatation ($)	17,000	32,000	49,000	69,000	0 (useful anchor)

* assumes 10 - 25 units

Note:

The total cost of the alkaline battery system is comparable to or greater than the cost of the lithium battery system except at depths less than 2000 m.

APPENDIX C

Tables of Mooring Component Characteristics

Details about components used for tomography moored systems construction are listed in Tables C.1 through C.8. The components listed are classed as lines, buoyancy, instruments and anchor. Characteristics given are type, size, shape, weights, breaking strengths, drag, working depth limit, cost, and source. The data presented has been compiled by the authors during a period from late 1979 to early 1981, mostly from manufacturers' specifications.

LINES

Type	Dia. Beneath Jacket, In.	Outside Dia. In.	Poly-Ethelene Jacket Thick. In.	Dry Weight LBS/FT	Dry Weight LBS/M	Wet Weight LBS/FT	Wet Weight LBS/M	Breaking Strength LBS	Drag per 1000 m (lbs per ft^2/sec^2) Normal	Drag per 1000 m (lbs per ft^2/sec^2) Tangential
WIRE ROPE, 3 x 19 Seale, Amgal-Monitor AAA Steel		3/16	0	.0586	.1923	.0509	.167	4490	71.4	1.6
		1/4	0	.0997	.327	.0867	.284	7580	95.2	2.1
		5/16	0	.153	.502	.133	.436	11500	119.0	2.7
		3/8	0	.220	.722	.191	.627	16400	142.8	3.2
	11/64	.252	.032	.062	.203	.039	.128	3500	96.0	1.4
	3/16	.269	.032	.073	.240	.047	.154	4490	103.3	1.6
	1/4	.329	.032	.119	.390	.081	.266	7580	125.3	2.8
	5/16	.392	.032	.179	.587	.125	.410	11500	149.3	3.3
	3/8	.456	.032	.253	.830	.181	.594	16400	173.8	3.9
	7/16	.524	.032	.346	1.135	.250	.820	22600	199.6	4.5
	1/2	.682	.080	.482	1.581	.319	1.047	29000	259.8	5.8
	3/4	.941	.080	1.08	3.54	.774	2.54	64000	358.5	8.0
CHAIN, Galvanized Steel Proof Coil		1/4	0	.71	2.33	.62	2.03	6000	171	5.1
		3/8	0	1.58	5.2	1.4	4.6	12500	256	7.7
		1/2	0	2.75	9.0	2.4	7.9	21000	342	10.3
		3/4	0	5.95	19.5	5.2	17.0	45000	512	15.4
ELECTRO-MECHANICAL CABLE, Single Conductor			*							
	.169	.209	.020	.054	.177	.037	.121	2400	79.6	1.8
	.184	.224	.020	.074	.243	.051	.167	3500	85.3	1.9
	.220	.245	.025	.100	.328	.069	.226	4600	93.3	2.1
	.252	.302	.025	.130	.427	.090	.295	5600	115.0	2.6
*Thickness typical; must be custom-made.	.291	.355	.032	.175	.574	.127	.417	8800	135.2	3.0
	.315	.379	.032	.200	.656	.144	.472	10000	144.3	3.2
	.371	.435	.032	.270	.886	.199	.653	13000	165.7	3.7
	.417	.481	.032	.340	1.116	.244	.801	16700	183.2	4.1
Extrapolated →	.500	.660	.080	.480	1.575	.325	1.066	22800	251.4	5.6
	.750	.910	.080	1.1	3.5	.8	2.5	56200	346.6	7.7
NYLON ROPE		3/4	0	.145	.476	.014	.046	14200	286	6.0
		1 1/8	0	.340	1.116	.033	.108	33000	429	9.0
		1 3/4	0	.830	2.723	.080	.262	78000	667	14.0

Table C.1

LINES

TYPE		COST $/METER	SOURCE	REMARKS		
Wire Rope						
Plain	3/16	1.3				
	1/4	(1.8)	U S STEEL			
	5/16	(2.5)				
	3/8	(3.1)				
Jacketed	11/64	(1.8)		11/64 is AA grade		
	3/16	2.0				
	1/4	2.8	U S STEEL			
	5/16	(3.8)				
	3/8	(4.7)				
	7/16	(5.7)				
	1/2	(6.7)				
	3/4	(11.1)				
Chain	1/4	(2.8)		1175	Conservative Working Load, LBS.	
	3/8	6.2	C. G. EDWARDS	2450		
	1/2	(11.0)		4250		
	3/4	(24.8)		9125		
				Conductor	Armor	
E-M Cable, Single Conductor	.169	(2.5)		6.6	9.4	
	.184	2.7	ROCHESTER CORP.	10	6.1	NOT TORQUE-BALANCED.
	.220	2.7		6.6	4.4	(About 5 turns per 100
	.252	(3.1)		6.6	3.2	feet at 50% of breaking
	.291	(3.6)		6.6	2.5	tension)
	.315	3.9		2.8	2.3	
	.371	4.7	ROCHESTER CORP.	2.8	1.5	
	.417	4.9		2.8	1.2	
Extrapolated	.500	(6.2)		2.8	1.0	Extrapolated
	.750	(10.5)		2.8	0.6	
				OHMS/1000 FT.		
Nylon Rope	3/4	(5.0)	COLOMBIAN ROPE CO.			
	1 1/8	(7.5)				
	1 3/4	(11.6)				

Table C.2

BUOYANCY

TYPE	SIZE AND SHAPE	WEIGHT, LBS.		AREA ft^2		DRAG LBS. PER FT^2/SEC^2		WORKING DEPTH LIMIT METERS
		DRY	WET	NORMAL	TANG.	NORMAL	TANG.	
High-Performance Syntactic Foam:								
TG26	1 $ft.^3$	26	-38					5000
TG22	1 $ft.^3$	22	-42					2050
Syntactic Foam Buoy	90" dia x 45" high oblate	3650	-3500	25	44	12.5	26.5	2000
	66" x 66" octagonal modular	3650	-3500	25	30	20	24	
Surplus Steel Sphere								
SS28B	28.5" dia. sphere	130	-318	-	4.43	-	2.20	213
SS58	58" " "	680	-3000	-	18.35	-	9.12	106
Steel Sphere SS28	28" dia. sphere	140	-294	-	4.28	-	2.13	585
SS41	41" " "	404	-956	-	9.17	-	4.56	442
SS56	55.25" dia. sphere	1815	-1510	-	16.65	-	8.28	686
SS61	61.25" " "	2182	-2273	-	20.46	-	10.17	625
SS67	67.25" " "	2644	-3188	-	24.67	-	12.26	580
SS73	73.75" " "	4365	-3500	-	29.67	-	14.75	610
Hypothetical Steel Sphere	5.5' dia. sphere	3419	-2164	-	23.76	-	11.8	1000
Aluminum Sphere								
SA22	22" dia. sphere	84	-124	-	2.64	-	1.31	1067
SA44	44" " "	480	-1100	-	10.56	-	5.25	914
Glass Ball	17" OD (GB-204 HR-17)	46.25	-56	-		-	2.04	6700
	4 balls in 20" x 20" x 70" fairing	182	-210	2.8	9.7	3.2	0.8	

Table C.3

BUOYANCY

TYPE	COST $	$/ LB.BUOY.	SOURCE	REMARKS
Syntactic Foam				
TG26 TG22	$438/ft^3$	11.5	Emerson & Cuming	Standard shape is 6" x 12" x 24"
Syntactic Foam Buoy	28000 24000	8.0 6.9	Emerson & Cuming	$32.67\#/ft^3$ dry
Steel Sphere				
SS28B SS58	325 450	1.0 .15	ORE	Navy Surplus
Steel Sphere				
SS28 SS41 SS56 SS61 SS67 SS73	575 1250 4000 5000 6300 7000	2.0 1.31 2.6 2.2 2.0 2.0	ORE	
Steel Sphere, Hypothetical	9738	3.2	Appendix D	$39.25\#/ft^3$ dry
Aluminum Sphere				
SA22 SA44	1100 5000	8.9 4.5	ORE	
Glass Ball, 17" Faired 4-pak	250 1000	4.4 4.4	BENTHOS	Includes Hard Hat. Fairing weathervanes. Normal drag includes skin friction.

Table C.4

INSTRUMENTS

DESCRIPTION	SIZE AND SHAPE	WEIGHT, LBS. DRY	WEIGHT, LBS. WET	AREA FT^2 NORM.	AREA FT^2 TANG.	DRAG LBS. PER FT^2/SEC^2 NORM.	DRAG LBS. PER FT^2/SEC^2 TANG.	WORKING DEPTH LIMIT (METERS)
Long-Range Transmitter	3 parallel cylinders: 1' dia. x 20' 1' dia. x 14' 1' dia. x 14'	1500	500	24.2 to 52.2	163.89 (skin area) 3.75 (end area)	57.33	4.31	4000
LRT Power Source	19.0" dia. x 44.5" long	760	360	5.87	1.97	7.01	2.51	1000
(Lithium battery)	20.2" dia. x 45.1" "	1110	670	6.33	2.23	7.56	2.84	2000
with pressure vessel	21.5" dia. x 45.7" "	1520	1020	6.82	2.52	8.14	3.21	3000
	23.0" dia. x 46.3" "	2010	1450	7.40	2.89	8.84	3.69	4000
	24.7" dia. x 47.1" "	2620	1980	8.08	3.33	9.65	4.25	5000
Receiver/Processor	8" dia., 6' long cylinder	300	150	4.00	0.35	4.78	0.54	4000
Pop-Up Buoy	22" dia. sphere + small winch and antenna	230	-50	-	4.65	-	3.22	900
Sea-Link Release & Transponder, Analog	7.5" dia., 48" length cylinder on 1.7m rod	160	71	3.0	10.0	3.30	0.30	6000
Sea-Link Release & Transponder Digital Shallow	6.6" dia., 45" length	64	17					900
Sea-Link Release & Transponder Digital Deep	7.5" dia., 48" length	106	42					6000

Table C.5

__INSTRUMENTS__ *cost not included in mooring cost plots

DESCRIPTION	COST $	SOURCES	REMARKS
LRT	Unknown*	WHOI	Does __not__ include Lithium Battery with pressure vessel. (See below)
LRT Power Source (Lithium battery) with pressure vessel	70.5K 71.0K 71.5K 72.0K 72.5K	Appendix B	
R/P	Unknown*	WHOI	
PUB	Unknown*	CSDL	
Sea-Link Release & Transponder, Analog	10K*	EG&G	2-year life sub-marginal. Integration of release with LRT and R/P is preferred.
Sea-Link Release & Transponder, Digital	9.5K* 10K*	EG&G	Lithium battery powered, 30 months life. Integration of release with LRT and R/P is preferred.

Table C.6

ANCHOR MODULES

MATERIAL	SIZE + SHAPE	WEIGHT, LBS.		AREA FT^2		DRAG LBS. PER FT^2/SEC^2		DEPTH LIMIT
		DRY	WET	NORM.	TANG.	NORM.	TANG.	
Cast Iron	Cylinder	$490/ft^3$	$426/ft^3$					None
	1' high x 2.55' dia.	2500	2170	2.5	5.1	3.05	1.00	

Table C.7

ANCHOR MODULES

MATERIAL	COST	REMARKS
Cast Iron 2500#	22¢/lb. $550.00	Custom cast into cylinders (with central hole) at no charge. Assume 2500 lbs. maximum per cylinder to permit handling.

Table C.8

APPENDIX D

Design of Hypothetical Steel Sphere for Subsurface Buoyancy

Consider an ideal hollow, thin-walled sphere. Three of its properties are: Weight in air (W), Gross buoyancy (B) and maximum working depth in the ocean (Z). It is shown here that

$$W \; \alpha \; B \; Z \tag{D-1}$$

For the case of steel, this equation, and the consequent one for net buoyancy, are evaluated. A plot is made of air weight and cost, versus maximum working depth.

Gross buoyancy is given by the product of volume and seawater density:

$$B = \frac{4}{3} \pi \, r^3 \, \rho_w g \quad , \tag{D-2}$$

where r = sphere outside radius, inches

$\rho_w g$ = seawater density = 0.03709 lbs/in.^{3} (on average)

$$B = 0.1554 \, r^3 \text{ lbs.} \tag{D-3}$$

For a thin sphere of thickness t ,

$$W = 4 \pi \, r^2 t \rho_m g \quad , \tag{D-4}$$

where $\rho_m g$ = material density = 0.28 lbs/in.^{3} for steel.

The maximum working pressure of this sphere is given by,

$$p = \frac{2t\sigma}{r} \quad \text{, neglecting buckling (see below)} \tag{D-5}$$

where p = pressure, psi

σ = working material stress, psi

= 27,000 psi for a practical steel (for example, ASTM A 285 Grade C Pressure Vessel Quality hot-rolled plate).

Using equation D-5 to substitute for t in equation D-4 gives,

$$W = 4 \pi r^3 p \frac{\rho_m g}{2\sigma}$$

$$= \left[\frac{4}{3} \pi r^3 \rho_w g\right] \frac{3 p \rho_m}{2 \sigma \rho_w} \qquad (D-6)$$

$$W = B \frac{3}{2} \frac{\rho_m}{\rho_w} \frac{p}{\sigma}$$

Using the numbers for steel:

$$\frac{W}{B} = 0.0004194 p \qquad (D-7)$$

where p is in psi

$$\frac{W}{B} = 0.0006125 Z \qquad (D-8)$$

where Z is in meters.

Net buoyancy is:

$$B_N = B - W$$

$$= W \left(\frac{1}{0.0006125Z} - 1 \right)$$

So:

$$\frac{W}{B_N} = \frac{Z}{1633 - Z} \qquad (D-9)$$

This is a useful result

Quoted prices of ORE steel sphere buoys between 56 and 22 inches diameter, vary between $2.50 and $5.00 per pound dry weight, respectively. We assume buoys would be purchased in quantity in a few large sizes.

Thus: $\$/W \approx 2$

or $$\$/B_N \approx 2Z/(1633 - Z) \qquad \text{(D-10)}$$

where B_N is in pounds

The last two equations are plotted in Figure D-1.

Buckling

The buckling pressure of a thin-walled sphere is given by

$$P = \frac{0.365\ E\ t^2}{r^2} \qquad \text{(D-11)}$$

For steel $E = 29 \times 10^6$ psi.
From equations (D-5) and (D-11) we see that buckling resistance governs sphere size at pressures below 275 psi (188 m), and allowable working stress governs sphere size at higher pressures. In our application, depth is always greater than 188 m. Lesser depths are not considered in Figure D-1.

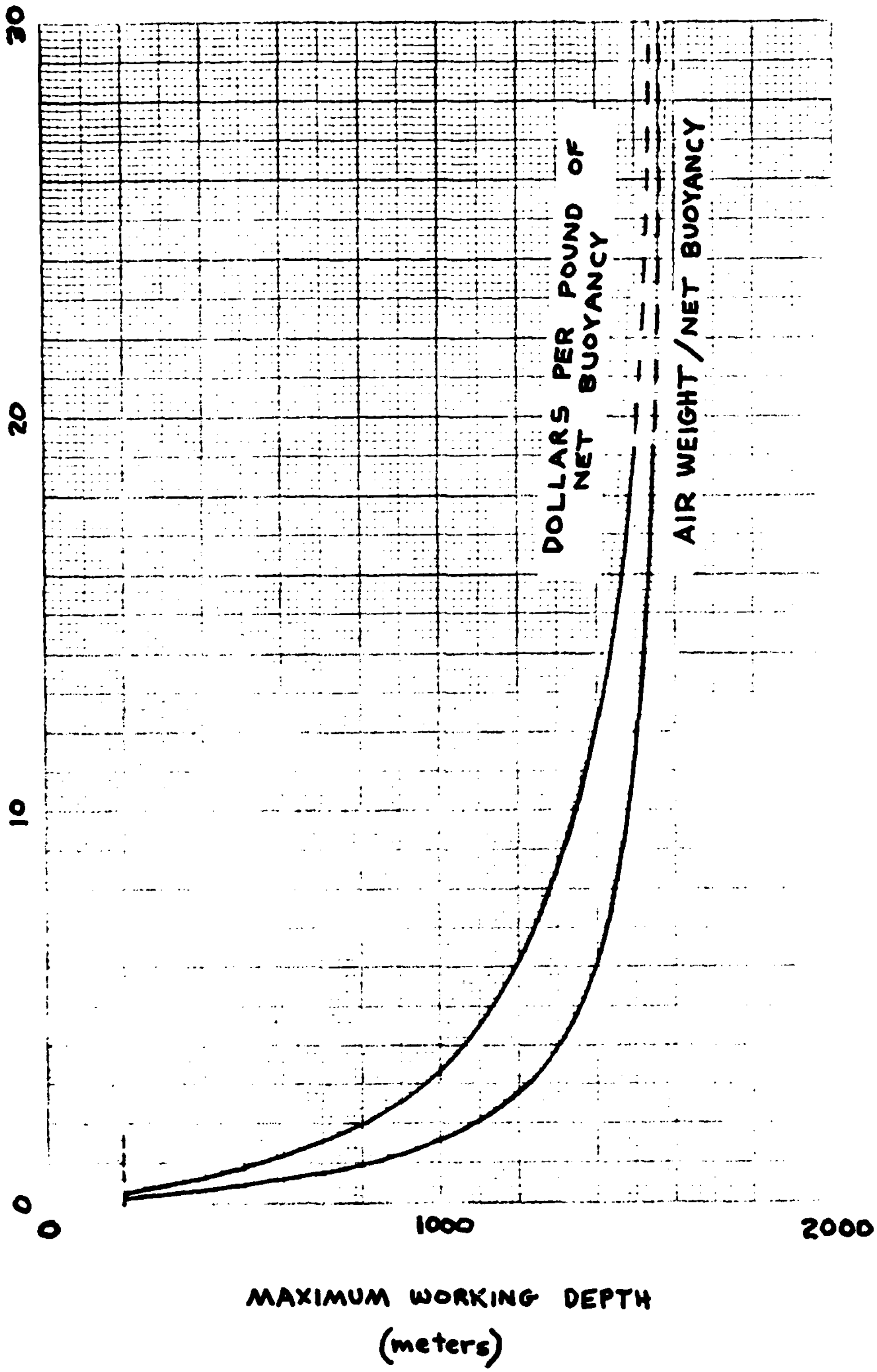

Figure D-1 Steel Sphere Buoyancy

REFERENCES

Munk, W. and C. Wunsch, 1979, "Ocean acoustic tomography: a scheme for large scale monitoring", Deep-Sea Research, Vol. 26A, pp. 123-161.

Chhabra, N.K., 1973, "Mooring Mechanics - A Comprehensive Computer Study, Volume 1", C.S. Draper Laboratory, Inc., Report R-775.

Chhabra, N.K., 1976, "Mooring Mechanics - A Comprehensive Computer Study, Volume 2", C.S. Draper Laboratory, Inc., Report R-1066.

Chhabra, N.K., J.M. Dahlen, and M.R. Froidevaux, 1974, "Mooring Dynamics Experiment: Determination of a Verified Dynamic Model of the WHOI Intermediate Mooring", C.S. Draper Laboratory, Inc., Report R-823.

Chhabra, N.K., 1974, "Verification of a computerized model for subsurface mooring dynamics using full-scale ocean test data". Marine Technology Society Tenth Annual Conference Proceedings.

Chhabra, N.K., 1977A,"Dynamic motions of a subsurface mooring system at anchor impact after its free fall to the ocean floor", C.S. Draper Laboratory, Inc., Report R-1079.

Chhabra, N.K., 1977B, "Correction of Vector-Averaging current meter records from the MODE-1 central mooring for the effects of low-frequency mooring line motion", Deep-Sea Research, 24, pp. 279-287.

Chhabra, N.K.,1979, "Dynamics of a tethered spar buoy system - validation using full-scale ocean test data". Proceedings of the specialty conference Civil Engineering in the Oceans IV, ASCE, pp. 208-223.

Dahlen, J.M., N.K. Chhabra, F.J. Siraco, and W.E. Toth, 1981, "The Pop-Up-Buoy (PUB)", C.S. Draper Laboratory, Inc., Report R-1480.

Garrett, Christopher and Walter Munk, 1972, "Space-Time Scales of Internal Waves," Geophysical Fluid Dynamics, Vol 3, pp. 225-264.

MANDATORY DISTRIBUTION LIST

FOR UNCLASSIFID TECHNICAL REPORTS, REPRINTS, & FINAL REPORTS
PUBLISHED BY OCEANOGRAPHIC CONTRACTORS
OF THE OCEAN SCIENCE AND TECHNOLOGY DIVISION
OF THE OFFICE OF NAVAL RESEARCH
(REVISED NOV 1978)

1 Deputy Under Secretary of Defense
(Research and Advanced Technology)
Military Assistant for Environmental Science
Room 3D129
Washington, DC 20301

Office of Naval Research
800 North Quincy Street
Arlington, VA 22217
3 ATTN: Code 483*
1 ATTN: Code 460
2 ATTN: 102B

1 ResRep (if any)

Commanding Officer
Naval Research Laboratory
Washington, DC 20375
6 ATTN: Library, Code 2627

12** Defense Documentation Center
Cameron Station
Alexandria, VA 22314
ATTN: DCA

Commander
Naval Oceanographic Office
NSTL Station
Bay St. Louis, MS 39522
1 ATTN: Code 8100
1 ATTN: Code 6000
1 ATTN: Code 3300

1 NODC/NOAA
Code D781
Wisconsin Avenue, N.W.
Washington, D.C. 20235

* Add one separate copy of
Form DD-1473

** Send with these 12 copies two completed forms DDC-50,
one self addressed back to the contractor, then the
other addressed to ONR, Code 480.

FILMED

6-8